

Effects of Coulomb collisions on lower hybrid drift waves inside a laboratory reconnection current sheet

Jongsoo Yoo,^{1, a)} Yibo Hu,² Jeong-Young Ji,³ Hantao Ji,^{1, 4} Masaaki Yamada,¹ Aaron Goodman,¹ Kendra Bergstedt,¹ William Fox,¹ and Andrew Alt¹

¹⁾*Princeton Plasma Physics Laboratory, Princeton, New Jersey 08543, USA.*

²⁾*School of Physical Science and Technology, Soochow University, Suzhou 215006, China.*

³⁾*Department of Physics, Utah State University, Logan, Utah 84322, USA.*

⁴⁾*Department of Astrophysical Sciences, Princeton University, Princeton, NJ 08544, USA.*

(Dated: 13 January 2022)

We have developed a local, linear theoretical model for lower hybrid drift waves that can be used for plasmas in the weakly collisional regime. Two cases with typical plasma and field parameters for the current sheet of the Magnetic Reconnection Experiment (MRX) have been studied. For a case with a low electron beta ($\beta_e = 0.25$, high guide field case), the quasi-electrostatic lower hybrid drift wave (ES-LHDW) is unstable, while the electromagnetic lower hybrid drift wave (EM-LHDW) has a positive growth rate for a high- β_e case ($\beta_e = 8.9$, low guide field case). For both cases, including effects of Coulomb collisions reduces the growth rate but collisional impacts on the dispersion and growth rate are limited ($\lesssim 20\%$).

^{a)}Electronic mail: jyoo@pppl.gov

I. INTRODUCTION

Magnetic reconnection converts magnetic energy into plasma thermal and flow energy via topological rearrangements of the magnetic field lines. Energy conversion processes during magnetic reconnection result in many free energy sources for waves and instabilities near the diffusion region such as strong gradients of the magnetic field and plasma parameters. Among them, the lower hybrid drift wave (LHDW) has been widely observed near the diffusion region in both space^{1–7} and laboratory plasmas^{8–10}. The free energy source of LHDWs is the cross-field current¹¹. The large density gradients near the separatrix can particularly be a free energy source by inducing a perpendicular current via a diamagnetic drift.

LHDWs have been a candidate for generating anomalous resistivity because it can interact differently with magnetized electrons and non-magnetized ions, resulting in momentum exchange between the two species^{7–9,12–16}. For reconnection with a negligible guide field, the fast-growing, short-wavelength ($k\rho_e \sim 1$; k is the magnitude of the wave vector \mathbf{k} , ρ_e is the electron gyroradius), quasi-electrostatic LHDW (ES-LHDW) is found to be localized at the edge of the current sheet⁸ due to the stabilization by the high plasma beta (β)¹⁷. On the other hand, the long-wavelength ($k\sqrt{\rho_e\rho_i} \sim 1$; ρ_i is the ion gyroradius), electromagnetic LHDW (EM-LHDW) that propagates obliquely to the magnetic field exists in the electron diffusion region⁹. However, extensive efforts via numerical particle-in-cell (PIC) simulations^{15,16} show that the electromagnetic LHDW (EM-LHDW) does not play an important role in fast reconnection and electron energization near the electron diffusion region during antiparallel reconnection.

Recent observations by the Magnetospheric Multiscale (MMS) mission show that the ES-LHDW can be generated inside or near the electron diffusion region^{5–7}, when there is a sizable guide field. The ES-LHDW can drive electron heating and vortical flows⁶ near the electron diffusion region. Moreover, the ES-LHDW is capable of generating anomalous drag between electrons and ions⁷.

Motivated by these observations, Yoo *et al.*⁷ have developed a local, linear theoretical model that explains dynamics of both ES- and EM-LHDWs in the presence of a guide field. This model is based on collisionless closures for the electron heat flux with the assumption of a gyrotrropic electron pressure tensor. Results from the model agree with activities of the ES- and EM-LHDWs inside a current sheet at the magnetopause⁷.

In laboratory experiments such as the Magnetic Reconnection Experiment (MRX), effects of

Collisional effects on lower hybrid drift waves

Coulomb collisions on magnetic reconnection and electron heating are not negligible. The classical Spitzer resistivity¹⁸, for example, can balance the reconnection electric field in the collisional regime and can even account for 10 – 20 % of that in the collisionless regime^{19,20}. This indicates that Coulomb collisions may also affect the dynamics of LHDWs in laboratory plasmas.

These collisional effects on LHDWs have not been considered previously, even though LHDWs in the reconnection current sheet have been extensively studied via theoretical analyses and numerical simulations^{11,14,21–23}. This paper provides the first quantitative study of the effects of Coulomb collisions on LHDWs. Through this model, we can address how the dynamics of LHDWs in laboratory plasmas are different from those in collisionless plasmas and when collisional effects become important. To include effects from collisions, we have advanced the previous models^{7,24} by using closures of the electron heat flux, heat generated by collisions, and resistivity that can be used for plasmas with arbitrary collisionality^{25,26}. For a self-consistent modeling of the heat flux and energy conservation, we also have allowed a first-order perturbation of the perpendicular electron temperature (T_{e1}^\perp), which was set to be zero in a previous model by Yoo *et al.*⁷. Unlike previous models, the zeroth-order electron temperature anisotropy is not allowed in the current model because the available closures were developed under the assumption of isotropic electron pressure at equilibrium. Except these changes, all other assumptions are the same: we used a kinetic equation for unmagnetized ions, fluid equations for electrons, and a gyrotrropic pressure tensor for electrons.

This linear model can be used to quantify the effects of LHDWs on electron heating and reconnection dynamics in weakly-collisional plasmas; with measured wave amplitudes and quasi-linear arguments, wave-associated anomalous terms and heat generated by collisions with ions can be directly estimated. It should be noted that the wave-associated heating power cannot be estimated by collisionless models.

In Section II, we explain the theoretical model for LHDWs in a local geometry. Then, in Section III, we numerically calculate dispersion relations of LHDWs for two cases. The biggest difference in the two cases is the value of electron beta, β_e . For the low- β_e case, which represents conditions near the electron diffusion region during reconnection with a strong guide field, the ES-LHDW is unstable. For the high- β_e case, which represents conditions in the same region but with a negligible guide field, the EM-LHDW has positive growth rates. In both cases, collisional effects on LHDWs with typical MRX parameters are not significant ($\lesssim 20\%$). Finally, in Section IV, we discuss the results and propose future research.

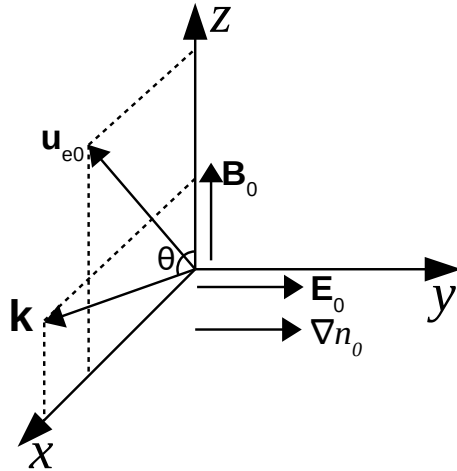


FIG. 1. Geometry of the local theory for the LHDW dispersion calculation. We are working in the ion rest frame with the z direction toward the equilibrium magnetic field (\mathbf{B}_0) and the y direction along the density gradient direction. Due to the force balance, the equilibrium electric field \mathbf{E}_0 is also along the y direction. The equilibrium electron flow velocity \mathbf{u}_{e0} and wave vector \mathbf{k} reside on the $x-z$ plane. The angle between \mathbf{k} and \mathbf{B}_0 is given by θ .

II. DERIVATION OF THE DISPERSION RELATION

Figure 1 shows the geometry of our local theoretical model for a lower hybrid drift wave (LHDW) inside a current sheet. Here the subscript 0 indicates equilibrium quantities. We chose the ion rest frame, and electrons have velocity (\mathbf{u}_{e0}) on the $x-z$ plane. The equilibrium magnetic field is along the z direction and the density gradient direction is along the y direction. In this model, there is neither equilibrium temperature gradient nor ion temperature anisotropy. The equilibrium electron temperature is also assumed to be isotropic, but anisotropy is allowed in the perturbed electron temperature. The wave vector (\mathbf{k}) lies on the $x-z$ plane due to our assumption of negligible k_y . Thus, our theoretical model is local and valid only when the wavelength of the LHDW is much smaller than the thickness of the current sheet in the y direction²⁴.

To balance the force associated with the pressure (density) gradient, there is an equilibrium electric field along the y direction. By using the ion and electron force balance equations, the

Collisional effects on lower hybrid drift waves

equilibrium electric field E_0 can be expressed in terms of other plasma parameters. From the ion force balance along the y direction, we have

$$en_0E_0 = T_{i0} \frac{dn_0}{dy} = \varepsilon n_0 T_{i0}, \quad (1)$$

where n_0 is the equilibrium density, T_{i0} is the equilibrium ion temperature, and $\varepsilon = (dn_0/dy)/n_0$ is the inverse of the density gradient scale. From the y component of the electron momentum equation, we have

$$-en_0(E_0 - u_{e0x}B_0) = T_{e0} \frac{dn_0}{dy}, \quad (2)$$

where u_{e0x} is the x component of the equilibrium electron flow velocity and T_{e0} is the equilibrium electron temperature. Then, the equilibrium electric field is

$$E_0 = \frac{T_{i0}}{T_{e0} + T_{i0}} u_{e0x} B_0. \quad (3)$$

The inverse of the gradient scale is given by

$$\varepsilon = \frac{eu_{e0x}B_0}{T_{e0} + T_{i0}}. \quad (4)$$

Note that Eqns. 3 and 4 are the same as those in the collisionless model in Yoo *et al.*⁷, because the resistivity term is zero along the y direction.

All perturbed quantities have a normal mode decomposition proportional to $\exp[i(\mathbf{k} \cdot \mathbf{x} - \omega t)]$ with the wave vector $\mathbf{k} = (k_{\perp}, 0, k_{\parallel})$. Here, the subscript 1 indicates perturbed quantities. For the dispersion relation, Maxwell's equations without the displacement current term are used:

$$\mathbf{k} \times (\mathbf{k} \times \mathbf{E}_1) = -i\omega\mu_0\mathbf{J}_1. \quad (5)$$

The displacement current term is ignored because the phase velocity of the wave is much smaller than the speed of light.

Assuming the equilibrium ion distribution function to be locally Maxwellian, the perturbed ion current density (\mathbf{J}_{i1}) is given by²⁴

$$\mathbf{J}_{i1} = -\frac{in_0e^2}{m_i k v_{ti}} \left[Z(\zeta) \mathbf{E}_1 + \frac{Z''(\mathbf{E}_1 \cdot \hat{\mathbf{k}})}{2} \hat{\mathbf{k}} - i \left(\frac{\varepsilon}{2k} \right) Z'' E_{1y} \hat{\mathbf{k}} \right], \quad (6)$$

where m_i is the ion mass, $v_{ti} = \sqrt{2T_{i0}/m_i}$ is the ion thermal speed, $\zeta = \omega/k v_{ti}$, and $Z(\zeta)$ is the plasma dispersion function. This is from a perturbed Vlasov equation for unmagnetized ions. This means that any dynamics slower than the ion cyclotron frequency have been ignored, including

Collisional effects on lower hybrid drift waves

collisional effects on ion dynamics. In our regime of interest, the ion collision frequency is smaller than the ion cyclotron frequency. The perturbed ion temperature can be also obtained, which is

$$T_{i1} = \frac{ie}{k} \left[\mathbf{E}_1 \cdot \hat{\mathbf{k}} \left(2Z' + \frac{Z'''}{4} \right) - iE_{1y} \left(\frac{\epsilon}{k} \right) \left(Z' + \frac{Z'''}{4} \right) \right]. \quad (7)$$

The perturbed electron current density \mathbf{J}_{e1} is obtained from fluid equations. This is different from the classical formulation of LHDWs, where the kinetic (Vlasov) equation is used for electron dynamics^{17,27,28}. Since electrons are magnetized, a gyrotropic electron pressure tensor is assumed. In this case, the 3 + 1 fluid model (n , \mathbf{u} , p^{\parallel} , and p^{\perp} ; p^{\parallel} and p^{\perp} are the parallel and perpendicular pressure, respectively) is appropriate²⁵. In this fluid model, off-diagonal terms of the electron pressure tensor are ignored.

The first order electron momentum equation is given by

$$im_en_0(\omega - \mathbf{k} \cdot \mathbf{u}_{e0})\mathbf{u}_{e1} = i\mathbf{k} \cdot \mathbf{P}_{e1} + en_0(\mathbf{E}_1 + \mathbf{u}_{e1} \times \mathbf{B}_0 + \mathbf{u}_{e0} \times \mathbf{B}_1) + e(\mathbf{E}_0 + \mathbf{u}_{e0} \times \mathbf{B}_0)n_{e1} - \mathbf{R}_{e1}, \quad (8)$$

where \mathbf{P}_{e1} is the perturbed electron pressure tensor and \mathbf{R}_{e1} is the perturbed resistivity. The perturbed electron density n_{e1} is given by the electron continuity equation, which is

$$(\omega - \mathbf{k} \cdot \mathbf{u}_{e0})n_{e1} = (\mathbf{k} \cdot \mathbf{u}_{e1} - i\epsilon u_{e1y})n_0. \quad (9)$$

To close the momentum equation, we need closures for \mathbf{P}_{e1} and \mathbf{R}_{e1} . For \mathbf{P}_{e1} , we only need closures for p_{e1}^{\perp} and p_{e1}^{\parallel} , since we assume a gyrotropic pressure tensor as mentioned earlier. To obtain p_{e1}^{\perp} and p_{e1}^{\parallel} , we start from the following kinetic equation:

$$\frac{\partial f_e}{\partial t} + \mathbf{v} \cdot \nabla f_e - \frac{e}{m_e}(\mathbf{E} + \mathbf{v} \times \mathbf{B}) \cdot \frac{\partial f_e}{\partial \mathbf{v}} = C(f_e), \quad (10)$$

where f_e is the electron distribution function and $C(f_e)$ is the collision operator. First, multiplying the kinetic equation with $m_e(v_z - u_{ez})^2$ and integrating over the velocity space yields

$$\frac{\partial p_e^{\parallel}}{\partial t} + \nabla \cdot (\mathbf{u}_e p_e^{\parallel}) + \nabla \cdot \mathbf{q}_e^{\parallel} + 2 \frac{\partial u_{ez}}{\partial z} p_e^{\parallel} = C_e^{\parallel}, \quad (11)$$

where

$$p_e^{\parallel} = m_e \int (v_z - u_{ez})^2 f_e d\mathbf{v}, \quad (12)$$

$$\mathbf{q}_e^{\parallel} = m_e \int (\mathbf{v} - \mathbf{u}_e)(v_z - u_{ez})^2 f_e d\mathbf{v}, \quad (13)$$

$$C_e^{\parallel} = \int C(f_e) m_e (\mathbf{v} - \mathbf{u}_e)^2 d\mathbf{v}. \quad (14)$$

Collisional effects on lower hybrid drift waves

Similarly, multiplying the kinetic equation with $m_e[(v_x - u_{ex})^2 + (v_y - u_{ey})^2]/2$ and integrating over the velocity space yields

$$\frac{\partial p_e^\perp}{\partial t} + \nabla \cdot (\mathbf{u}_e p_e^\perp) + \nabla \cdot \mathbf{q}_e^\perp + \left(\frac{\partial u_{ex}}{\partial x} + \frac{\partial u_{ey}}{\partial y} \right) p_e^\perp = C_e^\perp, \quad (15)$$

where

$$p_e^\perp = m_e \int \frac{1}{2} [(v_x - u_{ex})^2 + (v_y - u_{ey})^2] f_e d\mathbf{v}, \quad (16)$$

$$\mathbf{q}_e^\perp = m_e \int \frac{1}{2} [(v_x - u_{ex})^2 + (v_y - u_{ey})^2] (\mathbf{v} - \mathbf{u}_e) f_e d\mathbf{v}, \quad (17)$$

$$C_e^\perp = \int \frac{1}{2} C(f_e) [(v_x - u_{ex})^2 + (v_y - u_{ey})^2] d\mathbf{v}. \quad (18)$$

Linearizing Eqn. 11 yields

$$-i\omega p_{e1}^\parallel + \epsilon u_{e1y} n_0 T_{e0} + i(\mathbf{k} \cdot \mathbf{u}_0) p_{e1}^\parallel + i(\mathbf{k} \cdot \mathbf{u}_{e1}) n_0 T_{e0} + i\mathbf{k} \cdot \mathbf{q}_{e1}^\parallel + 2ik_\parallel u_{e1z} n_0 T_{e0} = C_{e1}^\parallel. \quad (19)$$

By using $p_{e1}^\parallel = n_{e1} T_{e0} + n_0 T_{e1}^\parallel$ and Eqn. 9, Eqn. 19 can be written as

$$i(\omega - \mathbf{k} \cdot \mathbf{u}_0) n_0 T_{e1}^\parallel = i\mathbf{k} \cdot \mathbf{q}_{e1}^\parallel + 2ik_\parallel u_{e1z} n_0 T_{e0} - C_{e1}^\parallel. \quad (20)$$

Similarly, linearizing Eqn. 15 yields

$$i(\omega - \mathbf{k} \cdot \mathbf{u}_0) n_0 T_{e1}^\perp = i\mathbf{k} \cdot \mathbf{q}_{e1}^\perp + ik_\perp u_{e1x} n_0 T_{e0} - C_{e1}^\perp. \quad (21)$$

We now need fluid closures for $\mathbf{q}_{e1}^\parallel$, \mathbf{q}_{e1}^\perp , C_{e1}^\parallel , and C_{e1}^\perp . First, the 3 + 1 fluid model gives us⁷

$$\mathbf{q}_e^\parallel = \frac{\hat{z}}{m_e \omega_{ce}} \times \left(p_e^\parallel \nabla T_e + T_e \nabla p_e^\parallel - \frac{T_e}{2} \nabla \pi_e^\parallel - T_e^\parallel \nabla p_e^\perp \right) + q_{ez}^\parallel \hat{z}, \quad (22)$$

where $\omega_{ce} = eB_0/m_e$, $\pi_e^\parallel = 2(p_e^\parallel - p_e^\perp)/3$ and $T_e^\parallel = p_e^\parallel/n_e$. After linearization, the x component of $\mathbf{q}_{e1}^\parallel$ is

$$q_{e1x}^\parallel = \frac{2T_{e0}}{3(T_{e0} + T_{i0})} n_0 u_{e0x} (T_{e1}^\parallel - T_{e1}^\perp) = r_{te} n_0 u_{e0x} (T_{e1}^\parallel - T_{e1}^\perp), \quad (23)$$

where $r_{te} = 2T_{e0}/3(T_{e0} + T_{i0})$. For \mathbf{q}_e^\perp , we derive a closure in Appendix A, which can be written as

$$\mathbf{q}_e^\perp = \frac{\hat{z}}{m_e \omega_{ce}} \times \left[\left(-\frac{5}{6} p_e^\parallel + \frac{17}{6} p_e^\perp \right) \nabla T_e - \left(\frac{2}{9} T_e^\parallel + \frac{4}{9} T_e^\perp \right) \nabla p_e^\parallel + \left(\frac{8}{9} T_e^\parallel - \frac{2}{9} T_e^\perp \right) \nabla p_e^\perp \right] + q_{ez}^\perp \hat{z}, \quad (24)$$

Collisional effects on lower hybrid drift waves

After linearization, the x component of $\mathbf{q}_{\text{e1}}^\perp$ is

$$q_{\text{e1}x}^\perp = -\frac{2T_{\text{e0}}}{3(T_{\text{e0}}+T_{\text{i0}})}n_0u_{\text{e0}x}(T_{\text{e1}}^\parallel - T_{\text{e1}}^\perp) = -r_{\text{te}}n_0u_{\text{e0}x}(T_{\text{e1}}^\parallel - T_{\text{e1}}^\perp). \quad (25)$$

For $q_{\text{e1}z}^\parallel$ and $q_{\text{e1}z}^\perp$, we employ a closure for plasmas with arbitrary collisionality, which can be written as²⁵

$$q_{\text{e1}z}^\parallel = \frac{6}{5}h_{\text{e1}}^\parallel + \sigma_{\text{e1}}^\parallel, \quad (26)$$

$$q_{\text{e1}z}^\perp = \frac{2}{5}h_{\text{e1}}^\parallel - \frac{1}{2}\sigma_{\text{e1}}^\parallel, \quad (27)$$

where

$$h_{\text{e1}}^\parallel = -\frac{1}{2}i\bar{k}_\parallel\bar{K}_{hh}n_0v_{\text{te}}T_{\text{e1}}^* + i\bar{k}_\parallel\bar{K}_{h\sigma}v_{\text{te}}\pi_{\text{e1}}^\parallel + \bar{K}_{hR}n_0T_{\text{e0}}(u_{\text{e1}z} - u_{\text{i1}z}) + i\bar{K}_{hS}v_{\text{te}}\pi_{\text{e1}}^\parallel, \quad (28)$$

$$\sigma_{\text{e1}}^\parallel = \frac{4}{3}i\bar{k}_\parallel\bar{K}_{h\sigma}n_0v_{\text{te}}T_{\text{e1}}^* - i\bar{k}_\parallel\bar{K}_{\sigma\sigma}v_{\text{te}}\pi_{\text{e1}}^\parallel + \bar{K}_{\sigma R}n_0T_{\text{e0}}(u_{\text{e1}z} - u_{\text{i1}z}) + i\bar{K}_{\sigma S}v_{\text{te}}\pi_{\text{e1}}^\parallel. \quad (29)$$

Here $T_{\text{e1}}^* = T_{\text{e1}} + 2\pi_{\text{e1}}^\parallel/5n_0$, $v_{\text{te}} = \sqrt{2T_{\text{e0}}/m_{\text{e}}}$ is the electron thermal speed, and $\bar{k}_\parallel = k_\parallel\lambda_c$ is the normalized parallel wave number. The electron collision length is defined as $\lambda_c \equiv v_{\text{te}}\tau_{\text{ee}}$, and the electron-electron collision time τ_{ee} is given by

$$\tau_{\text{ee}} = \frac{6\sqrt{2}\pi^{3/2}\epsilon_0^2\sqrt{m_{\text{e}}}T_{\text{e0}}^{3/2}}{n_0e^4\ln\Lambda_{\text{ee}}}, \quad (30)$$

where $\ln\Lambda_{\text{ee}}$ is the Coulomb logarithm for electron-electron collisions and ϵ_0 is the permittivity of free space. In Eqns. 28 and 29, \bar{K}_{AB} represents a kernel function that is obtained from a 6400 moment solution²⁵. The kernel function \bar{K}_{AB} has the following form:

$$\bar{K}_{AB} = \frac{a\bar{k}_\parallel^\alpha}{1 + d_1\bar{k}_\parallel^\delta + d_2\bar{k}_\parallel^{2\delta} + d_3\bar{k}_\parallel^{3\delta} + d_4\bar{k}_\parallel^{4\delta} + d_5\bar{k}_\parallel^{5\delta} + d_6\bar{k}_\parallel^{6\delta}}, \quad (31)$$

where values of coefficients such as a , α , and δ in Eqn. 31 are given in Table 1 in Ji and Joseph²⁵. For a negative \bar{k}_\parallel , $\bar{K}_{AB}(\bar{k}_\parallel) = \bar{K}_{AB}(-\bar{k}_\parallel)$ if $\alpha = 0$ or $\alpha = 2$. When $\alpha = 1$, $\bar{K}_{AB}(\bar{k}_\parallel) = -\bar{K}_{AB}(-\bar{k}_\parallel)$. These closures are consistent with those of Hammett and Perkins²⁹ in the collisionless limit, and they become consistent with those of Braginskii³⁰ in the collisional limit.

The heat generated by the collision terms C_{e1}^\parallel and C_{e1}^\perp also needs a closure, and can be written as

$$C_{\text{e1}}^\parallel = \frac{2}{3}Q_{\text{e1}} + S_{\text{e1}}^\parallel, \quad (32)$$

$$C_{\text{e1}}^\perp = \frac{2}{3}Q_{\text{e1}} - \frac{1}{2}S_{\text{e1}}^\parallel, \quad (33)$$

Collisional effects on lower hybrid drift waves

where Q_e is the heat generated by collisions and S_e^\parallel is related to the temperature anisotropy²⁵. The closure for S_{e1}^\parallel is given by²⁵

$$S_{e1}^\parallel = \frac{4}{3} \bar{k}_\parallel \bar{K}_{hs} \frac{n_0}{\tau_{ee}} T_{e1}^* + \frac{\bar{k}_\parallel}{\tau_{ee}} \bar{K}_{\sigma S} \pi_{e1}^\parallel + i \frac{8}{3} \bar{K}_{RS} \frac{n_0 T_{e0}}{v_{te} \tau_{ee}} (u_{e1z} - u_{i1z}) - \frac{2.05 - \bar{K}_{SS}}{\tau_{ee}} \pi_{e1}^\parallel. \quad (34)$$

The heat generated by collisions can be written as²⁶

$$Q_e = 3 \frac{m_e n_e}{m_i \tau_{ei}} (T_i - T_e) - \mathbf{u}_{ei} \cdot \mathbf{R}_e, \quad (35)$$

where τ_{ei} is the electron-ion collision time and $\mathbf{u}_{ei} = \mathbf{u}_e - \mathbf{u}_i$ is the relative flow velocity between electrons and ions. Assuming the ion charge status Z_i is unity, τ_{ei} is

$$\tau_{ei} = \frac{6\sqrt{2}\pi^{3/2}\epsilon_0^2\sqrt{m_e}T_{e0}^{3/2}}{n_0 e^4 \ln \Lambda_{ei}}, \quad (36)$$

where $\ln \Lambda_{ei}$ is the Coulomb logarithm for electron-ion collisions. Linearizing Q_e yields

$$Q_{e1} = 3 \frac{m_e n_{e1}}{m_i \tau_{ei}} (T_{i0} - T_{e0}) + 3 \frac{m_e n_0}{m_i \tau_{ei}} (T_{i1} - T_{e1}) - \mathbf{u}_{e0} \cdot \mathbf{R}_{e1} - \mathbf{u}_{ei1} \cdot \mathbf{R}_{e0}. \quad (37)$$

We also need an expression for the resistivity. Since there is no temperature gradient in the equilibrium quantities, the zeroth order resistivity \mathbf{R}_{e0} can be written as²⁶

$$\mathbf{R}_{e0} = -\alpha^\parallel \frac{m_e n_0}{\tau_{ei}} u_{e0z} \hat{\mathbf{z}} - \alpha^\perp \frac{m_e n_0}{\tau_{ei}} u_{e0x} \hat{\mathbf{x}}. \quad (38)$$

For $Z_i = 1$, the two coefficients are²⁶

$$\alpha^\parallel = 0.504, \quad (39)$$

$$\alpha^\perp = 1 - \frac{1.46r + 1.06}{r^{\frac{5}{3}} - 0.081r^{\frac{4}{3}} + 2.97r + 2.13}, \quad (40)$$

where $r = \omega_{ce} \tau_{ee}$. There are additional terms in \mathbf{R}_{e1} since temperature gradients exist in the first order. The parallel (z) component of \mathbf{R}_{e1} is²⁵

$$R_{e1}^\parallel = -i \frac{\bar{k}_\parallel \bar{K}_{hR}}{v_{te} \tau_{ee}} n_0 T_{e1}^* - i \frac{3}{4} \frac{\bar{k}_\parallel \bar{K}_{\sigma R}}{v_{te} \tau_{ee}} \pi_{e1}^\parallel - (1 - \bar{K}_{RR}) \frac{n_0 m_e}{\tau_{ee}} u_{ei1z} + i \frac{2 \bar{K}_{RS}}{v_{te} \tau_{ee}} \pi_{e1}^\parallel. \quad (41)$$

Eqn. 41 can be written as

$$R_{e1}^\parallel = -i k_\parallel n_0 \gamma_{ez}^\parallel T_{e1}^\parallel - i k_\parallel n_0 \gamma_{ez}^\perp T_{e1}^\perp - (m_e n_0 / \tau_{ee}) (1 - \bar{K}_{RR}) u_{ei1z}, \quad (42)$$

where

$$\gamma_{ez}^\parallel = \frac{3}{5} \bar{K}_{hR} + \frac{1}{2} \bar{K}_{\sigma R} - \frac{4 \bar{K}_{RS}}{3 \bar{k}_\parallel}, \quad (43)$$

$$\gamma_{ez}^\perp = \frac{2}{5}\bar{K}_{hR} - \frac{1}{2}\bar{K}_{\sigma R} + \frac{4\bar{K}_{RS}}{3\bar{k}_\parallel}. \quad (44)$$

The x component of \mathbf{R}_{e1} is²⁶

$$R_{e1}^\perp = -\alpha^\perp \frac{m_e n_0}{\tau_{ei}} u_{ei1x} - \alpha^\perp \frac{m_e u_{e0x}}{\tau_{ei}} n_{e1} - ik_\perp \beta^\perp n_0 T_{e1}, \quad (45)$$

where β^\perp for $Z_i = 1$ is given by²⁶

$$\beta^\perp = \frac{6.33r + 2.47}{r^{\frac{8}{3}} + 2.75r^{\frac{7}{3}} + 3.99r^2 + 5.31r^{\frac{5}{3}} + 8.23r + 3.52}. \quad (46)$$

Finally, the y component of \mathbf{R}_{e1} is given by $R_{e1}^\times = \alpha^\times m_e n_0 u_{ei1y} / \tau_{ei}$. Here the coefficient α^\times for $Z_i = 1$ is²⁶

$$\alpha^\times = \frac{r(2.53r + 0.81)}{r^{\frac{8}{3}} + 2.54r^{\frac{7}{3}} + 6.14r^2 + 7.35r^{\frac{5}{3}} + 11.22r + 4.09}. \quad (47)$$

With these closures, the first-order momentum equation (Eqn. 8) can be used to obtain the perturbed electron current density \mathbf{J}_{e1} . Then, the Maxwell equation (Eqn. 5) can be written as

$$\begin{pmatrix} D_{xx} & D_{xy} & D_{xz} \\ D_{yx} & D_{yy} & D_{yz} \\ D_{zx} & D_{zy} & D_{zz} \end{pmatrix} \begin{pmatrix} E_{1x} \\ E_{1y} \\ E_{1z} \end{pmatrix} = 0. \quad (48)$$

The detailed derivation of each component of tensor \mathbf{D} can be found in Appendix B.

III. COLLISIONAL EFFECTS ON THE DISPERSION

Dispersion relations for the lower hybrid drift waves are obtained from $|\mathbf{D}| = 0$, where $|\mathbf{D}|$ is the determinant of the tensor \mathbf{D} ; from this equation, the normalized angular frequency Ω is computed numerically for the given \mathbf{k} and θ . Required input parameters are B_0 , n_0 , T_{e0} , T_{i0} , u_{e0z} , and u_{e0x} . In addition, the ion mass has to be specified.

Compared to the previous collisionless model in Yoo *et al.*⁷, there are two significant changes in the current model: the inclusion of the first-order perturbation of the perpendicular electron temperature (T_{e1}^\perp) and the use of collisional closures. To understand the effects of each change, we obtain dispersion relations from four different models – (i) the collisionless model in Ref. Yoo *et al.*⁷, (ii) a model with collisional closures but without T_{e1}^\perp , (iii) the current model in the collisionless limit $\tau_{ee} \rightarrow \infty$, and (iv) the current model.

First, we obtain dispersion relations with typical plasma and field parameters near the electron diffusion region of the Magnetic Reconnection Experiment (MRX) during reconnection with a

guide field; $B_0 = 180$ Gauss, $n_0 = 2 \times 10^{13}$ cm $^{-3}$, $T_{e0} = T_{i0} = 10$ eV, $u_{e0z} = -130$ km/s, and $u_{e0x} = 50$ km/s. Here the ion species is singly-ionized helium. Justified by previous measurements in MRX^{19,31}, we assume that $Z_i = 1$. With these parameters, $\tau_{ee}\omega_{ce} = 157$, β_e is 0.25 and V_A is 44 km/s. Note that u_{e0x} exceeds V_A , which is a necessary condition for LHDWs to have large growth rates.

Figure 2 shows dispersion relations from the four models. Left (right) panels are contour plots of the real (imaginary) part of the angular frequency as a function of $k\rho_e$ and θ . Here $\rho_e = v_{te}/\omega_{ce}$ is the electron gyroradius. From now on, ω represents the real part of the angular frequency and γ represents the imaginary part. Both ω and γ are normalized to the (angular) lower hybrid frequency, ω_{LH} . All four models are qualitatively similar, showing strong growth rates ($\gamma \lesssim 0.6\omega_{LH}$) for the quasi-electrostatic lower hybrid drift wave (ES-LHDW). The ES-LHDW propagates almost perpendicular to \mathbf{B}_0 ($\theta \sim 90^\circ$) with $\omega \lesssim \omega_{LH}$. The peak growth rate occurs at $k\rho_e \sim 0.7$ and $\theta \sim 91^\circ$. Here $k\rho_e \sim 0.7$ corresponds to $\lambda \sim 0.6$ cm. These similarities among the four models indicate that the effects of Coulomb collisions on the ES-LHDW are limited for typical MRX parameters. Moreover, inclusion of T_{e1}^\perp also has a limited impact on the dispersion.

For better comparison between the four models, the dispersion relation and growth rate of the ES-LHDW are presented in Fig. 3 for $\theta = 91^\circ$. It is worth noting that including Coulomb collisions decreases the growth rate γ . This is understandable since collisions decrease the reaction of electrons to the external perturbation, such that they reduce the positive feedback from the plasma. The change in ω is not straightforward but is related to frequency shift due to additional terms of u_{e1x} and u_{e1z} . For example, the parallel force balance equation Eqn. B.48 has the resistivity R_{e1}^\parallel , which adds additional terms in α_{ez} in Eqn. B.50. These additional terms can cause a shift in ω (note that α_{ez} has a dependency on ω via α_e).

It is interesting to see that including T_{e1}^\perp in the electron dynamics decreases both ω and γ of the ES-LHDW. Interpreting this trend is complicated, because T_{e1}^\perp impacts both the x and z components of the electron momentum equation. For the x component, the first term ($ik_\perp n_0 T_{e1}^\perp$) on the right side of Eqn. B.55, which is the perturbed perpendicular electron pressure gradient term, directly contains T_{e1}^\perp . For the parallel momentum balance of Eqn. B.48, T_{e1}^\perp affects T_{e1}^\parallel via q_{e1x}^\parallel in Eqn. 23. The parallel resistivity (Eqn. 42) also has a term with T_{e1}^\perp ($-ik_\parallel n_0 \gamma_{ez}^\perp T_{e1}^\perp$).

The dispersion relation is calculated after setting $\gamma_{ez}^\perp = 0$ to remove contributions from T_{e1}^\perp in the z component of the electron force balance equation. As shown in Fig. 4, this change (green line) decreases ω and increases γ , compared to the reference case with T_{e1}^\perp (red line). Changes in

Collisional effects on lower hybrid drift waves

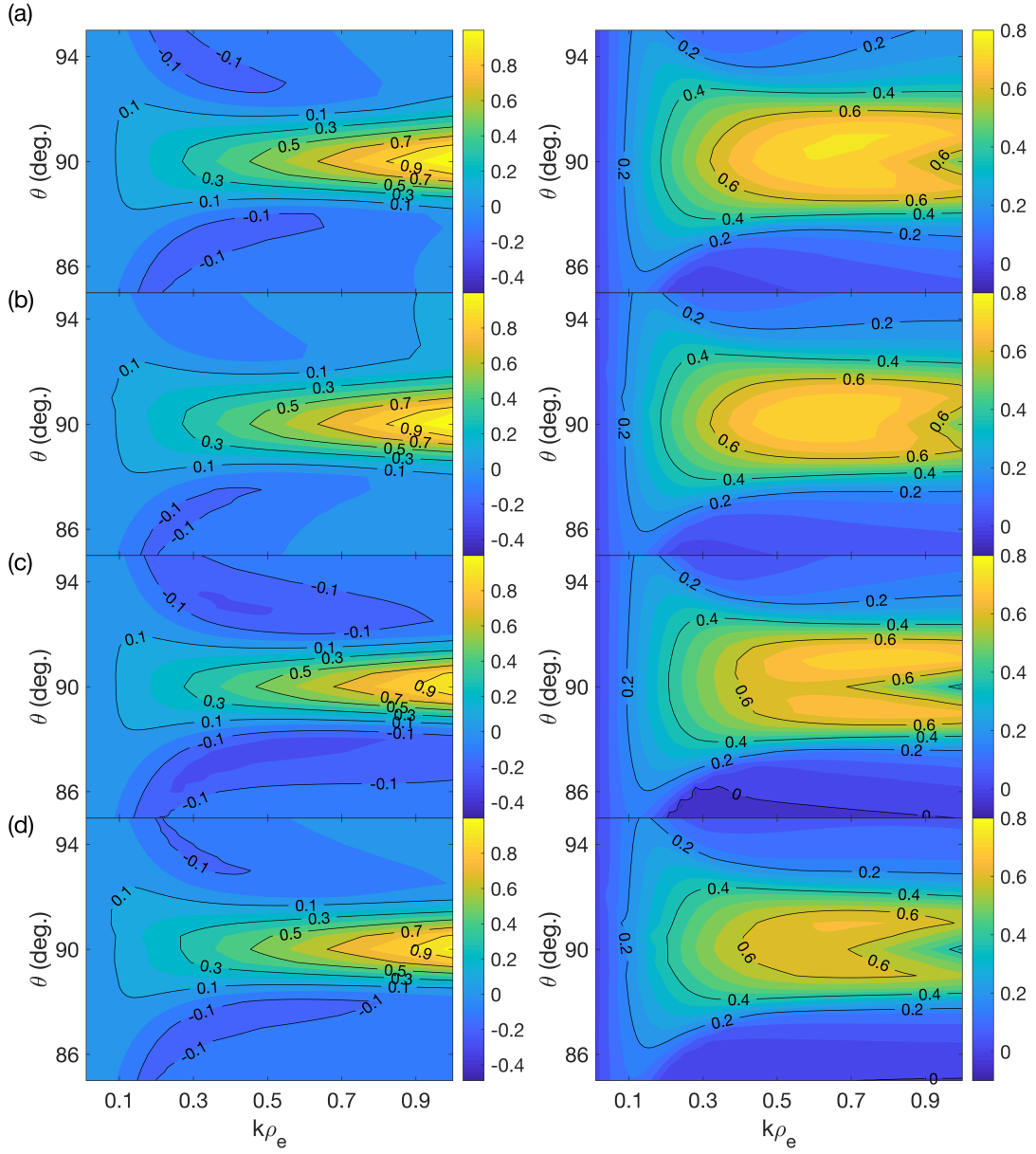


FIG. 2. Dispersion relation of the LHDW with typical MRX parameters near the electron diffusion region with a high guide field. Left (right) panels show the real (imaginary) part of the angular frequency as a function of k and θ . (a) Collisionless model without T_{el}^{\perp} . (b) Collisional model without T_{el}^{\perp} . (c) Model with T_{el}^{\perp} in the collisionless limit ($\tau_{\text{ee}} \rightarrow \infty$). (d) Collisional model with T_{el}^{\perp} (the most complete model). Results from the four models qualitatively agree with each other; the quasi-electrostatic LHDW that propagates almost perpendicular to \mathbf{B}_0 is unstable. The maximum growth rate appears around $k\rho_e \sim 0.7$ and $\theta \sim 91^\circ$. The growth rate of the mode decreases with collisional effects (b,d), compared to the corresponding collisionless cases (a,c).

Collisional effects on lower hybrid drift waves

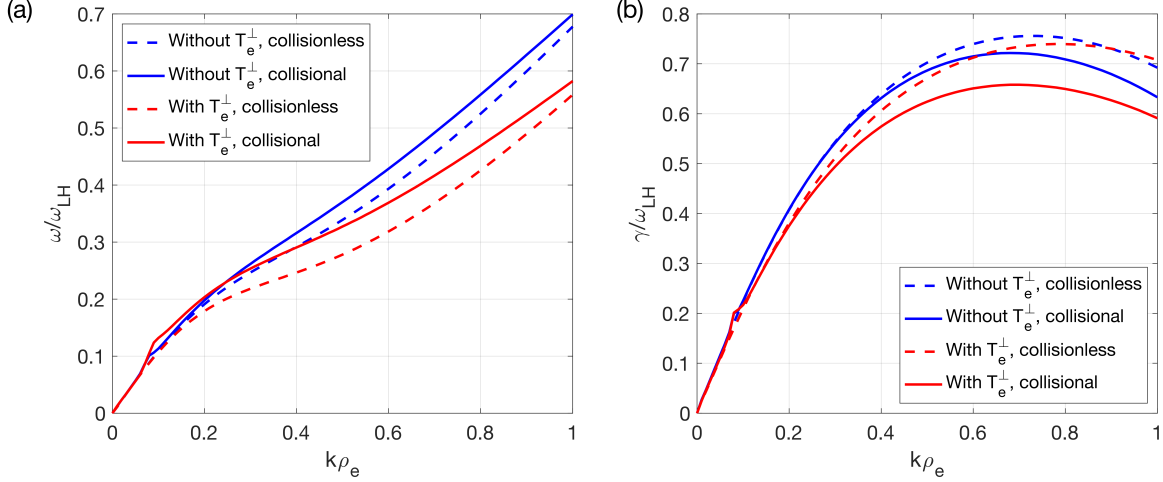


FIG. 3. 1D dispersion relation of the ES-LHDW for $\theta = 91^\circ$. (a) $\omega/\omega_{\text{LH}}$ as a function of $k\rho_e$. Including collisional effects (solid lines) increases the real frequency, while models with T_{e}^\perp (red lines) have lower ω . (b) $\gamma/\omega_{\text{LH}}$ as a function of $k\rho_e$. Collisional effects (solid lines) decrease γ , compared to results from the corresponding collisionless cases (dashed lines).

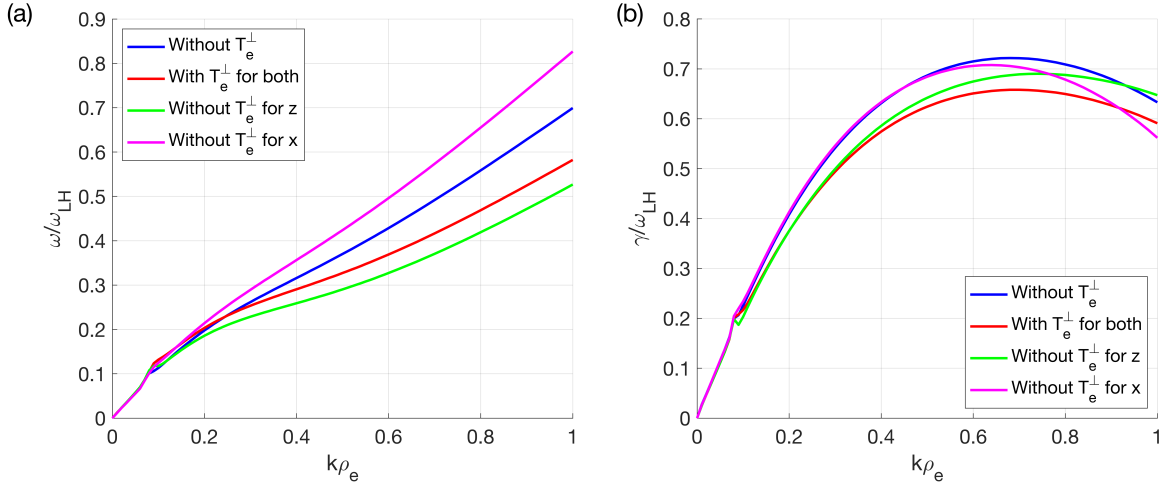


FIG. 4. 1D dispersion relation of the ES-LHDW for $\theta = 91^\circ$. (a) $\omega/\omega_{\text{LH}}$ as a function of $k\rho_e$ for four cases with collisional effects. The blue (red) line indicates the reference case without (with) T_{e}^\perp . If T_{e}^\perp is removed from the x component of the electron momentum equation (cyan line), ω becomes significantly larger. Removing the contribution from T_{e}^\perp in the z component of the electron momentum equation (green line), on the other hand, reduces ω . (b) $\gamma/\omega_{\text{LH}}$ as a function of $k\rho_e$ for four cases with collisional effects. Effects of T_{e}^\perp on γ are not important, as all four cases show similar values.

ω and γ are not significant.

The change in ω with T_{e1}^\perp is caused by the $ik_\perp n_0 T_{e1}^\perp$ term in the x component of the electron momentum equation. As shown in Fig. 4 (a), without the term (magenta line), ω increases significantly compared to the reference case with T_{e1}^\perp (red line). Removing the $ik_\perp n_0 T_{e1}^\perp$ term also increases γ for most values of k . Again, these changes are caused by the frequency shift due to the additional term with u_{e1x} ; from Eqns. B.55 and B.35, the inertial term effectively changes from $im_e n_0 (\omega - \mathbf{k} \cdot \mathbf{u}_{e0}) u_{e1x}$ to $im_e n_0 (\omega - \mathbf{k} \cdot \mathbf{u}_{e0} - 0.5 \bar{c}_{ux}^\perp k_\perp v_{te}) u_{e1x}$.

We have repeated the dispersion calculation for the electromagnetic, long-wavelength LHDW (EM-LHDW) that propagates obliquely to \mathbf{B}_0 . The plasma and field parameters used for calculations are $B_0 = 30$ Gauss, $n_0 = 2 \times 10^{13}$ cm $^{-3}$, $T_{e0} = T_{i0} = 10$ eV, $u_{e0z} = -50$ km/s, and $u_{e0x} = 130$ km/s. Again, the ion species is singly-ionized helium and $Z_i = 1$. With these parameters, $\tau_{ee} \omega_{ce} = 26.2$, β_e is 8.9 and V_A is 7.3 km/s. These parameters represent typical MRX values near the electron diffusion region during reconnection with a negligible guide field.

As shown in Fig. 5, dispersion relations from the four models again qualitatively agree with each other; these models expect positive growth rates for the EM-LHDW. Models without T_{e1}^\perp have the maximum growth rate around $k\rho_e \sim 0.6$ and $\theta \sim 55^\circ$, while those with T_{e1}^\perp have the maximum growth rate around $k\rho_e \sim 0.5$ and $\theta \sim 50^\circ$. The wavelength with the largest growth rate is about 4 cm. It is interesting to see that all models expect that the mode has frequency significantly less than ω_{LH} in the ion rest frame. This agrees with measurements in MRX and numerical simulations that show that most of the power of the EM-LHDW exists below ω_{LH} ^{9,16}.

For comparison between the four models, ω and γ as a function of k for $\theta = 55^\circ$ are presented in Fig. 6. Similar to the ES-LHDW case, collisional effects decrease γ regardless of the existence of T_{e1}^\perp in the model. This is consistent with the aforementioned explanation; collisions decrease the reaction of electrons to the external perturbation, thereby decreasing the positive feedback. For the EM-LHDW, collisions generally decrease ω especially when T_{e1}^\perp is not included in the model (blue lines). Including T_{e1}^\perp further decreases both ω and γ for this mode (red lines).

IV. SUMMARY AND DISCUSSION

In summary, we have developed a local, linear model of LHDWs that includes effects of Coulomb collisions and T_{e1}^\perp . This model works best for plasmas with weak collisionality. Without collisions, some assumptions for the 3+1 model may not be valid, as the zeroth-order distribution

Collisional effects on lower hybrid drift waves

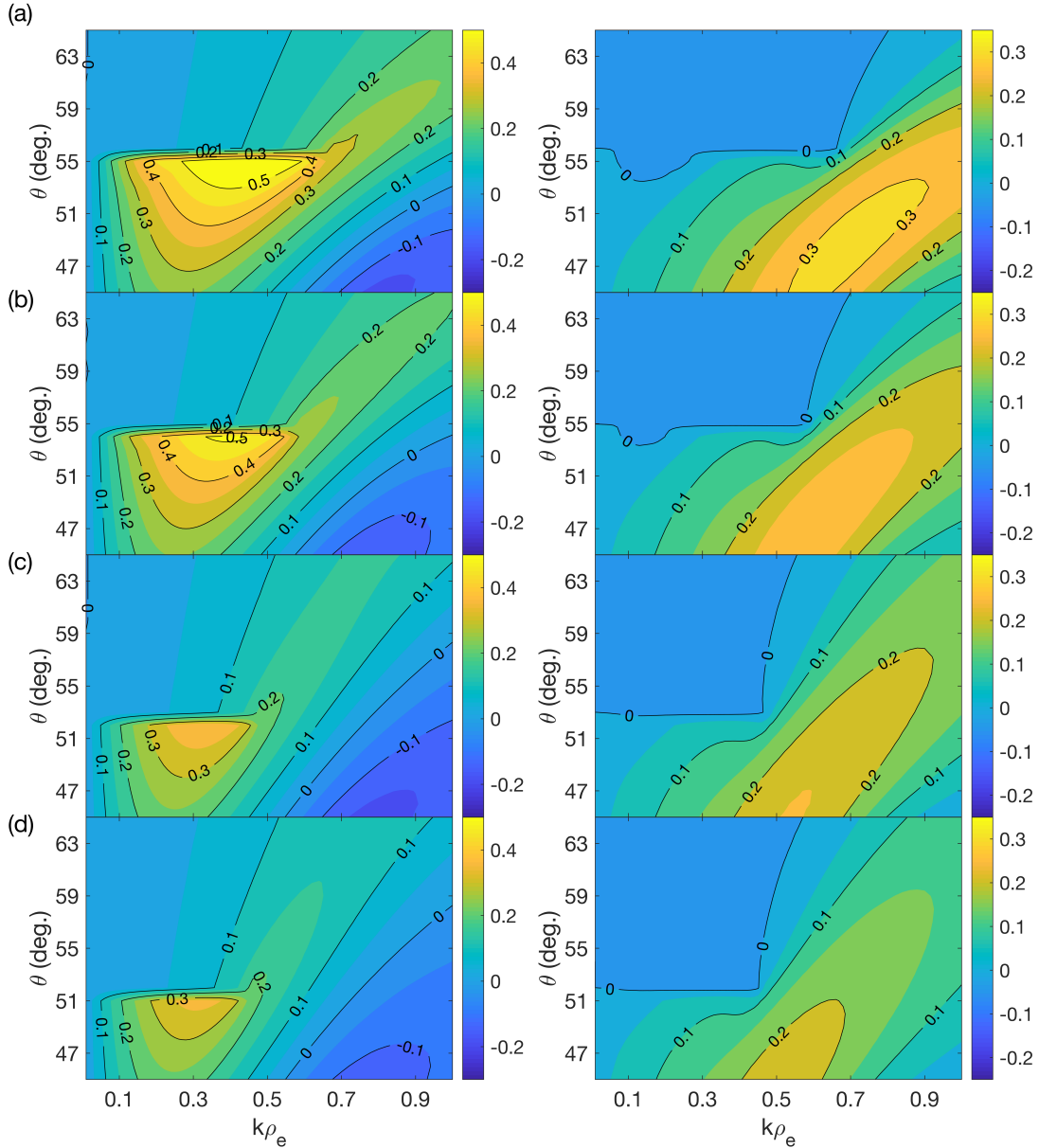


FIG. 5. Dispersion relation of the LHDW with typical MRX parameters near the electron diffusion region with a negligible guide field. Left (right) panels show the real (imaginary) part of the angular frequency as a function of k and θ . (a) Collisionless model without T_{e1}^\perp . (b) Collisional model without T_{e1}^\perp . (c) Model with T_{e1}^\perp in the collisionless limit ($\tau_{ee} \rightarrow \infty$). (d) Collisional model with T_{e1}^\perp (the most complete model). Again, results from the four models qualitatively agree with each other; the electromagnetic LHDW that propagates obliquely to \mathbf{B}_0 is unstable. The maximum growth rate appears around $k\rho_e \sim 0.5$ and $\theta \sim 50^\circ$. The growth rate of the mode decreases with collisional effects (b,d), compared to the corresponding collisionless cases (a,c).

Collisional effects on lower hybrid drift waves

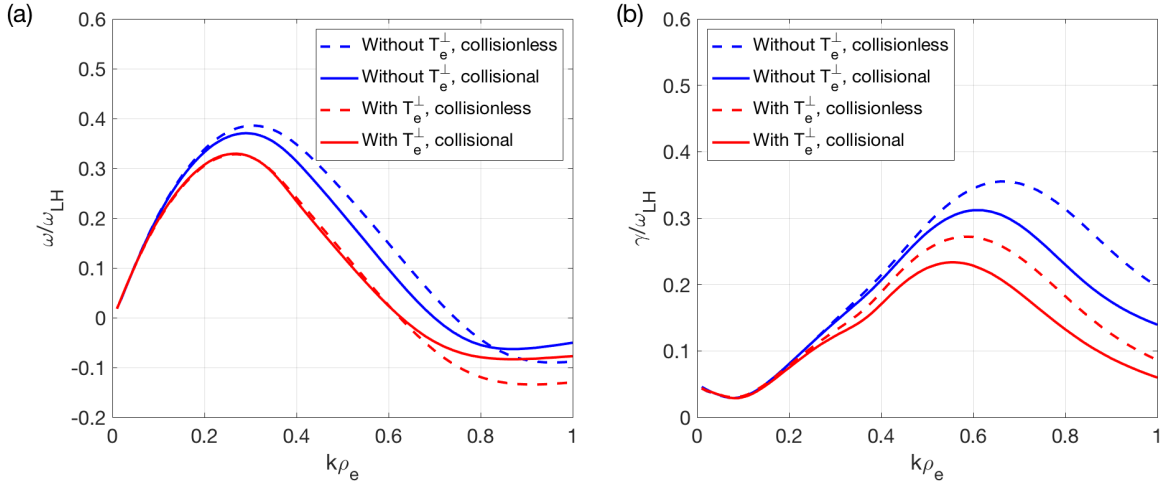


FIG. 6. 1D dispersion relation of the EM-LHDW for $\theta = 55^\circ$. (a) $\omega/\omega_{\text{LH}}$ as a function of $k\rho_e$. Models with $T_{\text{e}\perp}$ (red lines) have lower ω . The impact of Coulomb collisions on ω is negligible. (b) $\gamma/\omega_{\text{LH}}$ as a function of $k\rho_e$. Collisional effects (solid lines) decreases γ , compared to results from the corresponding collisionless cases (dashed lines).

function is not close to a Maxwellian. In addition, in the collisionless plasma, agyrotropy can be developed, while a gyrotropic electron pressure tensor is assumed in this model. For collisional plasmas, we need to consider the zeroth-order electric field along the x and z directions; for the zeroth-order electron force balance, additional components of \mathbf{E}_0 are needed to balance the zeroth-order resistivity $\mathbf{R}_{\text{e}0}$. If there are too many collisions, we need additional first-order terms ($eE_{0x}n_{\text{e}1}$ and $eE_{0z}n_{\text{e}1}$) in the x and z components of the electron momentum equation (Eqn. 8). From Eqn. 38, required equilibrium electric field components are given by $E_{0z} = -\alpha^{\parallel}B_0u_{\text{e}0z}/\omega_{\text{ce}}\tau_{\text{ei}}$ and $E_{0x} = -\alpha^{\perp}B_0u_{\text{e}0x}/\omega_{\text{ce}}\tau_{\text{ei}}$. From Eqn. 3, E_{0x}/E_0 is given by

$$\frac{E_{0x}}{E_0} = -\frac{\alpha^{\perp}T_{\text{e}0}}{T_{\text{e}0} + T_{\text{i}0}} \frac{1}{\omega_{\text{ce}}\tau_{\text{ei}}} \sim -\frac{1}{\omega_{\text{ce}}\tau_{\text{ee}}}, \quad (49)$$

because $\alpha_{\perp} \sim T_{\text{e}0}/(T_{\text{e}0} + T_{\text{i}0}) \sim 1$ and $\tau_{\text{ei}} \sim \tau_{\text{ee}}$ for $Z_i = 1$. This means that E_{0x} is negligible compared to E_0 , as long as electrons are fully magnetized ($\omega_{\text{ce}}\tau_{\text{ee}} \gg 1$), which is one of the basic assumptions of this model. From a similar argument, E_{0z} is also negligible unless $|u_{\text{e}0z}| \gg |u_{\text{e}0x}|$. For the two cases presented here, effects of both E_{0x} and E_{0z} are expected to be minimal since $|u_{\text{e}0z}| \sim |u_{\text{e}0x}|$ and $\omega_{\text{ce}}\tau_{\text{ee}} \gg 1$.

To verify this argument, we have calculated dispersion relations of LHDWs after including two additional terms ($eE_{0x}n_{\text{e}1}$ and $eE_{0z}n_{\text{e}1}$) and have found that impacts from these terms are actually

Collisional effects on lower hybrid drift waves

negligible. The basic reason for not including additional components of \mathbf{E}_0 in the current model is that including E_{0x} may require an additional electron flow component along the y direction, since there will be a corresponding $\mathbf{E} \times \mathbf{B}$ drift of electrons, while ions are unmagnetized. This means that collisions may impact the dynamics of LHDWs by changing the equilibrium itself. A future work will address this effect in a self-consistent manner. As the main purpose of the current study is to study collisional effects on LHDWs, we minimize other changes for simplicity. The parallel component of the equilibrium electric field E_{0z} , on the other hand, can be easily added in the model without creating complexity. Moreover, E_{0z} in the electron diffusion region during reconnection with a strong guide field may significantly exceed the value required to balance the classical resistivity³². In the future, we will study possible impacts of E_{0z} on LHDWs with values measured in MRX during guide field reconnection.

With this model, we have calculated two sets of LHDW dispersion relations for typical MRX parameters. The first case uses parameters from the electron diffusion region during reconnection with a significant guide field, while the second one uses those with a negligible guide field. Due to the presence of the guide field, the first case has a low electron beta ($\beta_e = 0.25$), such that the ES-LHDW is unstable in that region. For the second case ($\beta_e = 8.9$), on the other hand, the ES-LHDW is stabilized by the high beta effect¹⁷ and the EM-LHDW is unstable instead.

It will be interesting to study the critical value of β_e that determines whether the ES- or EM-LHDW is unstable. Initial studies show that the critical value is determined by the value of u_{e0x}/V_A ; for a relatively low (~ 1) value of u_{e0x}/V_A like the first case, β_e also has to be low ($\lesssim 0.5$) to have the ES-LHDW unstable. For a high value (> 10) of u_{e0x}/V_A , on the other hand, the ES-LHDW exists at the higher $\beta_e \sim 1$. We plan to conduct a statistical study with data from MMS and/or MRX, which will be compared to results from the current theoretical model.

Based on the two cases we have studied, collisional effects on LHDWs in typical MRX current sheets are limited. In both cases, including Coulomb collisions in the model decreases the growth rate. However, the difference in γ is relatively small ($\lesssim 20\%$). This is because the wavelengths of LHDWs (0.5–5 cm) are smaller than the mean free path of electrons (~ 10 cm) and electrons are fully magnetized ($\omega_{ce}\tau_{ee} \gg 1$) for these parameters.

To further investigate how collisions may impact on the dispersion relation, we have artificially varied τ_{ee} and τ_{ei} . For the ES-LHDW, artificially high collisions significantly affect the dispersion relation and the growth rate, as shown in Fig. 7 (a) and (b). When the collisions are enhanced by a factor of 5 (red dashed line), the real frequency becomes larger for $k\rho_e > 0.2$ than the reference

Collisional effects on lower hybrid drift waves

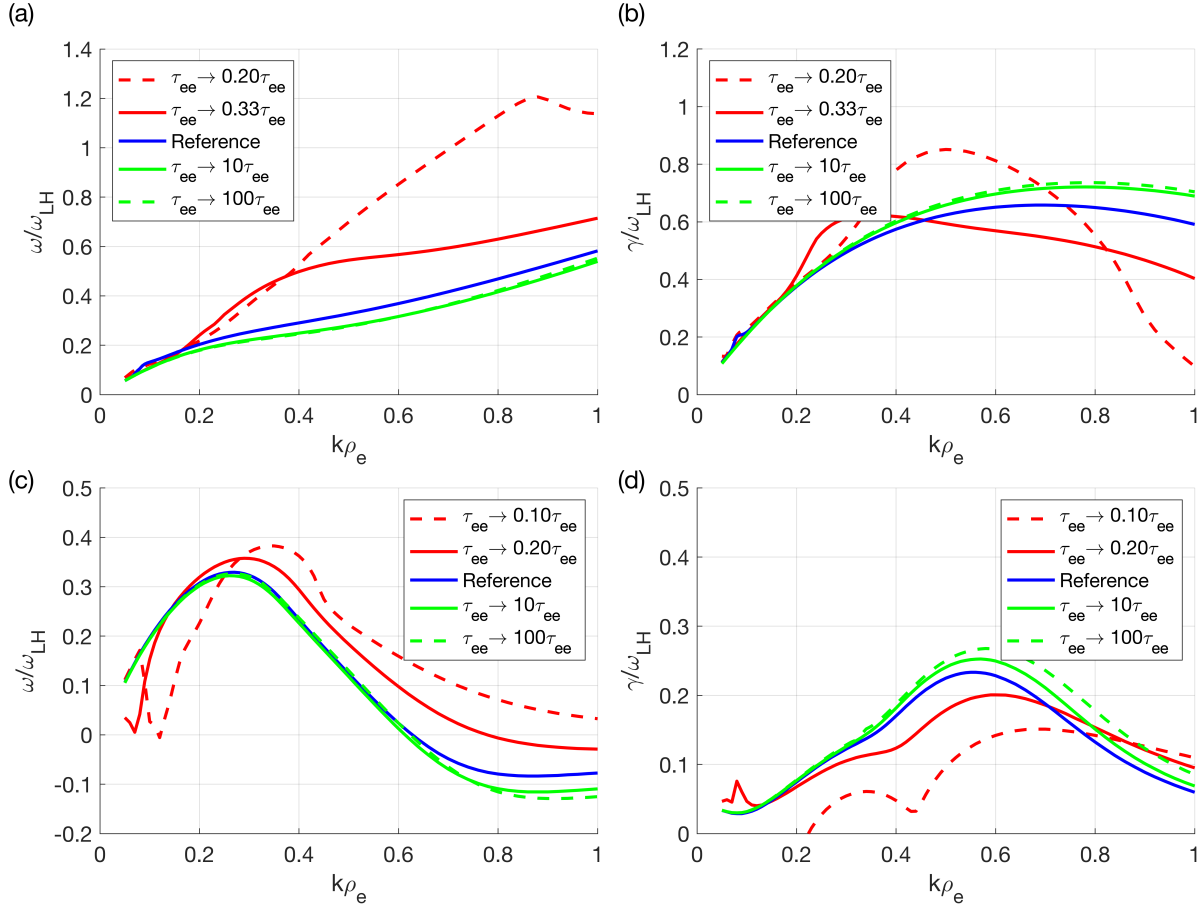


FIG. 7. 1D dispersion relations with various collisionalities for the two cases. (a) $\omega/\omega_{\text{LH}}$ as a function of $k\rho_e$ for the ES-LHDW case. When τ_{ee} is artificially decreased to $0.2\tau_{\text{ee}}$ (red dashed line), which means that collisions are enhanced by a factor of 5, there is a significant increase in ω when $k\rho_e > 0.4$. The same change is also applied to the other collision time, τ_{ei} . The blue line indicates the reference value without any change in the collision time. (b) $\gamma/\omega_{\text{LH}}$ as a function of $k\rho_e$ for the ES-LHDW case. When collisions are enhanced (red solid and dashed lines), there are noticeable changes in γ . (c) $\omega/\omega_{\text{LH}}$ as a function of $k\rho_e$ for the EM-LHDW case. When collisions are enhanced, there are large changes in the dispersion. (d) $\gamma/\omega_{\text{LH}}$ as a function of $k\rho_e$ for the EM-LHDW case. When collisions are enhanced (red solid and dashed lines), the growth rate with smaller $k\rho_e$ decreases notably.

value (blue solid line). There is also significant decrease in the growth rate for $k\rho_e > 0.7$. Changes in less collisional cases, on the other hand, (green solid and dashed lines) are minimal. With the reduced collision time ($\tau_{\text{ee}} \rightarrow 0.2\tau_{\text{ee}}$), the mean free path ($\tau_{\text{ee}}\nu_{\text{te}}$) becomes about 2 cm, which

Collisional effects on lower hybrid drift waves

corresponds to $k\rho_e \sim 0.2$. This supports the insertion that collisions have large impacts on modes with a wavelength comparable to the mean free path ($\lambda \sim 2\pi\tau_{ee}v_{te}$).

For the case of the EM-LHDW, effects from collisions become significant when collisions are enhanced by a factor of 5 or more ($\tau_{ee} \rightarrow 0.2\tau_{ee}$ and $\tau_{ei} \rightarrow 0.2\tau_{ei}$). As denoted by the red line in Fig. 7 (c), the overall shape of the dispersion relation changes noticeably, when τ_{ee} is reduced to $0.2\tau_{ee}$. The mean free path with $0.2\tau_{ee}$ is about 2 cm (the same electron temperature and density as the first case), and the change starts around $0.2k\rho_e$. When τ_{ee} reduces even further to $0.1\tau_{ee}$ (red dashed line), the deviation from the reference line starts around $0.1k\rho_e$. For both cases, there are also significant reductions in γ , as shown in Fig. 7 (d) especially for $k\rho_e < 0.7$.

This means that parameters for the two cases studied here are actually in the weakly collisional regime and that the dynamics of LHDWs are susceptible to collisional effects only when collisions are strong. For example, if the base electron temperature for both cases is 3 eV, the dispersion relation from this collisional model will be vastly different from that of the collisionless model.

Including T_{e1}^\perp in the model has limited impacts on the dispersion; it generally decreases the frequency and growth rate of LHDWs, but changes in ω and γ are less than 20 % for both cases. These changes mostly come from the additional pressure gradient term ($ik_\perp n_0 T_{e1}^\perp$) in the electron momentum equation along the x direction. This limited impact is related to the existence of Lorentz force terms along the perpendicular direction⁷; because of these terms, the electron force balance is less sensitive to the pressure gradient term along the perpendicular direction.

It should be noted that the current theoretical model ignores the global structure of the current sheet by assuming that there is no wave propagation along the density gradient direction (y direction in Fig. 1). To address the effects from the global current sheet structure, an eigenmode analysis^{21,33} or numerical simulations^{22,23} will have to be carried out, which will be one of our future works. In MRX, where the current sheet is actually broader ($\sim 10d_e$; d_e is electron skin depth), this local approximation is generally valid, as the length scale along the y direction is larger than the wavelength of LHDWs.

This model assumes that there is no equilibrium temperature gradient across the current sheet. In MRX, electrons are locally heated in the current sheet^{20,34}. However, inside the current sheet the temperature gradient is rather small, compared to that of density. Therefore, effects of the temperature gradient are expected to be negligible²⁴.

This study will provide a theoretical framework for quantifying anomalous terms and heating associated with LHDWs in MRX. With the solved dispersion relation, we can express every

fluctuating quantity in terms of a measurable quantity. For example, the first-order density perturbation (Eqn. B.81) can be expressed in terms of the fluctuation in the reconnection electric field (δE_{rec}) that can be measured with a probe^{8,35}. Then, the wave-associated anomalous drag term $D = -\langle \delta n_e \delta E_{\text{rec}} \rangle / \langle n_e \rangle$ ³⁶ can be estimated by measuring δE_{rec} . Here the assumption is that the linear relation holds, such that we can use $n_{e1} \sim \delta n_e$. Furthermore, this model can provide direct estimates of wave-associated heating in Eqn. 35 via the same quasi-linear argument. This estimate cannot be done with other collisionless models. In the future, we will establish quasi-linear calculations and conduct measurements of LHDWs in MRX to find out how LHDWs affect the electron and reconnection dynamics.

Appendix A: Derivation of the heat flux closure

From the kinetic equation in the $(t, \mathbf{r}, \mathbf{w} \equiv \mathbf{v} - \mathbf{V})$ coordinates (\mathbf{V} is the fluid velocity),

$$\frac{df}{dt} - (\mathbf{w} \cdot \nabla \mathbf{V}) \cdot \frac{\partial}{\partial \mathbf{w}} f + \nabla \cdot (\mathbf{w} f) + \frac{\partial}{\partial \mathbf{w}} \cdot (\mathbf{A} f) + \frac{q}{m} \mathbf{w} \times \mathbf{B} \cdot \frac{\partial}{\partial \mathbf{w}} f = C(f), \quad (\text{A.1})$$

where

$$\frac{d}{dt} = \frac{\partial}{\partial t} + \mathbf{V} \cdot \nabla, \quad (\text{A.2})$$

$$\mathbf{A} = \frac{1}{m} [\mathbf{F}_* + q(\mathbf{V} \times \mathbf{B})] - \frac{d\mathbf{V}}{dt}. \quad (\text{A.3})$$

For the p^{\parallel} fluid equation, we need to obtain the closure

$$\mathbf{q}^{\parallel} = \int d^3 v m w_{\parallel}^2 \mathbf{w} f = q_{\parallel}^{\parallel} \hat{z} + \mathbf{q}_{\perp}^{\parallel}, \quad (\text{A.4})$$

$$\mathbf{q} = \mathbf{h} = \int d^3 v \frac{1}{2} m w^2 \mathbf{w} f = h_{\parallel} \hat{z} + \mathbf{h}_{\perp}, \quad (\text{A.5})$$

where

$$q_{\parallel}^{\parallel} = \int d^3 v m w_{\parallel}^3 f = \frac{6}{5} h_{\parallel} + \sigma_{\parallel}, \quad (\text{A.6})$$

$$q_{\parallel}^{\perp} = \int d^3 v \frac{1}{2} m w_{\perp}^2 w_{\parallel} f = \frac{2}{5} h_{\parallel} - \frac{1}{2} \sigma_{\parallel}. \quad (\text{A.7})$$

have been obtained in Ji and Joseph²⁵ and the $\mathbf{q}_{\perp}^{\parallel}$ has been obtained in Yoo *et al.*⁷. Now we obtain

$$\mathbf{q}^{\perp} = \int d^3 v \frac{1}{2} m w_{\perp}^2 \mathbf{w} f = q_{\parallel}^{\perp} \hat{z} + \mathbf{q}_{\perp}^{\perp}. \quad (\text{A.8})$$

Note that \mathbf{q}^{\perp} can be obtained from

$$\mathbf{h}_{\perp} = \mathbf{q}_{\perp} = \int d^3 v \frac{1}{2} m w^2 \mathbf{w}_{\perp} f = \frac{1}{2} \mathbf{q}_{\perp}^{\parallel} + \mathbf{q}_{\perp}^{\perp}. \quad (\text{A.9})$$

Collisional effects on lower hybrid drift waves

We adopt the closure (transport) ordering $d/dt \approx 0$ and the linear response theory, linear in thermodynamic drives i.e. ∇T , ∇p_{\parallel} and ∇p_{\perp} .

We take the moments $\int d^3v \frac{1}{2} mw^2 \mathbf{w}$ of the kinetic equation:

$$\int d^3v \frac{1}{2} mw^2 \mathbf{w} \frac{df}{dt} = \frac{d}{dt} \mathbf{q} : \text{ignored by the closure ordering,}$$

$$\begin{aligned} \int d^3v \frac{1}{2} mw^2 \mathbf{w} (\mathbf{w} \cdot \nabla \mathbf{V}) \cdot \frac{\partial}{\partial \mathbf{w}} f &: \text{ignored by the linearization,} \\ \int d^3v \frac{1}{2} mw^2 \mathbf{w} \nabla \cdot (\mathbf{w} f) &= \nabla \cdot \left(\int d^3v \frac{1}{2} mw^2 \mathbf{w} \mathbf{w} f \right). \end{aligned}$$

We should decompose $\mathbf{w} \mathbf{w} \mathbf{w} \mathbf{w}$ into orthogonal polynomials (see Ji and Held³⁷) for the consistent truncation in the expansion of a distribution function.

$$\mathbf{c} = \frac{\mathbf{w}}{v_T} = \frac{\mathbf{w}}{\sqrt{2T/m}}. \quad (\text{A.10})$$

In terms of orthogonal basis

$$\begin{aligned} c^2 \mathbf{c} \mathbf{c} &= c^2 \left(\mathbf{c} \mathbf{c} - \frac{1}{3} c^2 \mathbf{I} \right) + \frac{1}{3} c^4 \mathbf{I} \\ &= \left(c^2 - \frac{7}{2} \right) \left(\mathbf{c} \mathbf{c} - \frac{1}{3} c^2 \mathbf{I} \right) + \frac{7}{2} \left(\mathbf{c} \mathbf{c} - \frac{1}{3} c^2 \mathbf{I} \right) + \frac{1}{3} c^4 \mathbf{I} \\ &= -\mathbf{p}^{21} + \frac{7}{2} \mathbf{p}^{20} + \frac{2}{3} \left(\frac{1}{2} c^4 - \frac{5}{2} c^2 + \frac{15}{8} \right) \mathbf{I} + \frac{2}{3} \left(\frac{5}{2} c^2 - \frac{15}{8} \right) \mathbf{I} \\ &= -\mathbf{p}^{21} + \frac{7}{2} \mathbf{p}^{20} + \frac{2}{3} \mathbf{p}^{02} \mathbf{I} + \left[\frac{5}{3} \left(c^2 - \frac{3}{2} \right) + \frac{5}{2} - \frac{5}{4} \right] \mathbf{I} \\ &= -\mathbf{p}^{21} + \frac{7}{2} \mathbf{p}^{20} + \frac{2}{3} \mathbf{p}^{02} \mathbf{I} + \left(-\frac{5}{3} \mathbf{p}^{01} + \frac{5}{4} \right) \mathbf{I}, \end{aligned} \quad (\text{A.11})$$

$$\begin{aligned} \int d\mathbf{v} \frac{1}{2} mw^2 \mathbf{w} \mathbf{w} f &\rightarrow \frac{1}{2} mv_T^4 \left[\frac{7}{2} \mathbf{p}^{20} + \left(-\frac{5}{3} \mathbf{p}^{01} + \frac{5}{4} \right) \mathbf{I} \right] \\ &= \frac{7}{2} \frac{1}{2} v_T^2 \boldsymbol{\pi} + \frac{1}{2} mv_T^4 \frac{5}{4} n \mathbf{I} \\ &= \frac{7}{2} \frac{T}{m} \boldsymbol{\pi} + \frac{5}{2} \frac{T}{m} p \mathbf{I} \\ &= \frac{7}{2} \frac{T}{m} \mathbf{p} - \frac{T}{m} p \mathbf{I}. \end{aligned} \quad (\text{A.12})$$

Hereafter \rightarrow will be used to drop \mathbf{b} terms which will be nullified by the $\mathbf{b} \times$ operation:

$$\nabla \cdot \boldsymbol{\pi} = \frac{3}{2} \mathbf{b} \partial_{\parallel} \pi_{\parallel} - \frac{1}{2} \nabla \pi_{\parallel} \rightarrow -\frac{1}{2} \nabla \pi_{\parallel}. \quad (\text{A.13})$$

Collisional effects on lower hybrid drift waves

For the $\frac{\partial}{\partial \mathbf{w}} \cdot (\mathbf{A}f)$ term

$$\mathbf{A} = \frac{1}{m} [\mathbf{F}_* + q(\mathbf{V} \times \mathbf{B})] - \frac{d\mathbf{V}}{dt} = \frac{1}{mn} (\nabla p + \nabla \cdot \boldsymbol{\pi}). \quad (\text{A.14})$$

$$\begin{aligned} \int d\mathbf{v} \frac{1}{2} mw^2 \mathbf{w} \frac{\partial}{\partial \mathbf{w}} \cdot (\mathbf{A}f) &= - \int d\mathbf{v} m \mathbf{A} \cdot \frac{\partial}{\partial \mathbf{w}} \left(\frac{1}{2} w^2 \mathbf{w} \right) f \\ &= - \int d\mathbf{v} m (\mathbf{A} \cdot \mathbf{w} \mathbf{w} + \frac{1}{2} w^2 \mathbf{A}) f \\ &= -\mathbf{p} \cdot \mathbf{A} - \frac{3}{2} p \mathbf{A} \\ &= -\mathbf{A} \cdot \boldsymbol{\pi} - \frac{5}{2} p \mathbf{A}. \end{aligned} \quad (\text{A.15})$$

All together $\nabla \cdot (\mathbf{w}f) + \frac{\partial}{\partial \mathbf{w}} \cdot (\mathbf{A}f)$

$$\begin{aligned} \mathbf{all} &= \nabla \cdot \left(\frac{7}{2} \frac{T}{m} \boldsymbol{\pi} + \frac{5}{2} \frac{T}{m} p \mathbf{l} \right) - \frac{1}{mn} (\nabla p + \nabla \cdot \boldsymbol{\pi}) \cdot \boldsymbol{\pi} - \frac{5}{2} p \frac{1}{mn} (\nabla p + \nabla \cdot \boldsymbol{\pi}) \\ &= \frac{7}{2m} (\nabla T \cdot \boldsymbol{\pi} + \underline{T \nabla \cdot \boldsymbol{\pi}}_1) + \frac{5}{2m} (p \nabla T + \underline{T \nabla p}_0) - \frac{1}{mn} (\nabla p + \nabla \cdot \boldsymbol{\pi}) \cdot \boldsymbol{\pi} - \frac{5}{2} p \frac{1}{mn} (\underline{\nabla p}_0 + \underline{\nabla \cdot \boldsymbol{\pi}}_1) \\ &= \frac{7}{2m} \nabla T \cdot \boldsymbol{\pi} + \frac{1}{m} T \nabla \cdot \boldsymbol{\pi} + \frac{5}{2m} p \nabla T - \frac{1}{mn} (\nabla p + \nabla \cdot \boldsymbol{\pi}) \cdot \boldsymbol{\pi}. \end{aligned} \quad (\text{A.16})$$

$$\begin{aligned} \int d^3v \frac{1}{2} mw^2 \mathbf{w} \frac{\partial}{\partial \mathbf{w}} \cdot (\mathbf{w} \times \mathbf{B}f) &= -\frac{1}{2} m \int d^3v (\mathbf{w} \times \mathbf{B}f) \cdot \frac{\partial}{\partial \mathbf{w}} (w^2 \mathbf{w}) \\ &= -\frac{1}{2} m \int d^3v (\mathbf{w} \times \mathbf{B}f) \cdot (2\mathbf{w} \mathbf{w} + w^2 \mathbf{l}) \\ &= -\frac{1}{2} m \int d^3v w^2 \mathbf{w} \times \mathbf{B}f \\ &= -\mathbf{h} \times \mathbf{B}. \end{aligned} \quad (\text{A.17})$$

$$\frac{q}{m} \int d^3v \frac{1}{2} mw^2 \mathbf{w} \frac{\partial}{\partial \mathbf{w}} \cdot (\mathbf{w} \times \mathbf{B}f) = -\Omega \mathbf{h} \times \hat{z}. \quad (\text{A.18})$$

The final equation becomes up to $\mathcal{O}(\Omega^0)$

$$(\text{terms dropped by closure ordering}) + \mathbf{all} + (\text{terms } \propto \mathbf{b}) - \Omega \mathbf{h} \times \hat{z} = (\text{collision terms } \propto \mathbf{b})$$

$$\begin{aligned} \mathbf{h}_\perp &= \frac{1}{\Omega} \hat{z} \times \mathbf{all} \\ \mathbf{h}_\perp &= \frac{1}{m\Omega} \mathbf{b} \times \left[\frac{5}{2m} \nabla T \cdot \boldsymbol{\pi} + \frac{1}{m} T \nabla \cdot \boldsymbol{\pi} + \frac{5}{2m} p \nabla T - \frac{1}{mn} (\nabla \cdot \boldsymbol{\pi}) \cdot \boldsymbol{\pi} \right]. \end{aligned} \quad (\text{A.19})$$

Since we are interested in \mathbf{q}_\perp up to $\mathcal{O}(\Omega^{-1})$, we consider only the CGL viscosity which is $\mathcal{O}(\Omega^0)$

$$\boldsymbol{\pi} = \frac{3}{2} \boldsymbol{\pi}_\parallel (\mathbf{b} \mathbf{b} - \frac{1}{3} \mathbf{l}), \quad (\text{A.20})$$

$$\begin{aligned}\nabla \cdot \boldsymbol{\pi} &= \frac{3}{2} \mathbf{b} \partial_{\parallel} \pi_{\parallel} - \frac{1}{2} \nabla \pi_{\parallel} \\ &= -\frac{1}{2} \nabla \pi_{\parallel} + \mathbf{b} \text{ terms},\end{aligned}\quad (\text{A.21})$$

and

$$\begin{aligned}(\nabla \cdot \boldsymbol{\pi}) \cdot \boldsymbol{\pi} &= \left(\frac{3}{2} \mathbf{b} \partial_{\parallel} \pi_{\parallel} - \frac{1}{2} \nabla \pi_{\parallel} \right) \cdot \frac{3}{2} \pi_{\parallel} (\mathbf{b} \mathbf{b} - \frac{1}{3} \mathbf{l}) \\ &= \frac{1}{4} \pi_{\parallel} \nabla \pi_{\parallel} + \mathbf{b} \text{ terms},\end{aligned}\quad (\text{A.22})$$

$$\begin{aligned}\mathbf{a} \mathbf{l} \mathbf{l} &= \frac{7}{2m} \nabla T \cdot \boldsymbol{\pi} + \frac{1}{m} T \nabla \cdot \boldsymbol{\pi} + \frac{5}{2m} p \nabla T - \frac{1}{mn} (\nabla p + \nabla \cdot \boldsymbol{\pi}) \cdot \boldsymbol{\pi} \\ &= -\frac{7}{4m} \pi_{\parallel} \nabla T - \frac{T}{2m} \nabla \pi_{\parallel} + \frac{5}{2m} p \nabla T + \frac{\pi_{\parallel}}{2mn} \nabla p - \frac{1}{4mn} \pi_{\parallel} \nabla \pi_{\parallel} + \mathbf{b} \text{ terms},\end{aligned}\quad (\text{A.23})$$

$$\mathbf{q}_{\perp} = \frac{1}{m\Omega} \mathbf{b} \times \left(-\frac{7}{4} \pi_{\parallel} \nabla T - \frac{T}{2} \nabla \pi_{\parallel} + \frac{5}{2} p \nabla T + \frac{\pi_{\parallel}}{2n} \nabla p - \frac{1}{4n} \pi_{\parallel} \nabla \pi_{\parallel} \right), \quad (\text{A.24})$$

$$\mathbf{q}_{\perp}^{\parallel} = \mathbf{q}_{\perp} - \frac{1}{2} \mathbf{q}_{\perp}^{\parallel}, \quad (\text{A.25})$$

where⁷

$$\mathbf{q}_{\perp}^{\parallel} = \frac{1}{m\Omega} \mathbf{b} \times \left(p^{\parallel} \nabla T + T \nabla p^{\parallel} - \frac{T}{2} \nabla \pi_{\parallel} - \frac{p^{\parallel}}{n} \nabla p^{\perp} \right). \quad (\text{A.26})$$

Finally,

$$\mathbf{q}^{\perp} = q_{\parallel}^{\perp} \hat{z} + \mathbf{q}_{\perp}^{\perp}. \quad (\text{A.27})$$

One can rewrite equations in terms of p^{\parallel} and p^{\perp} using

$$\pi_{\parallel} = \frac{2}{3} (p^{\parallel} - p^{\perp}), \quad (\text{A.28})$$

$$p = \frac{1}{3} (p^{\parallel} + 2p^{\perp}) = nT. \quad (\text{A.29})$$

Appendix B: Derivation of tensor D

In terms of $T_{\text{e1}}^{\parallel}$ and T_{e1}^{\perp} , $q_{\text{e1z}}^{\parallel}$ and q_{e1z}^{\perp} (Eqns. 26 and 27) can be expressed as

$$q_{\text{e1z}}^{\parallel} = -i \bar{c}_{q\parallel}^{\parallel} n_0 v_{\text{te}} T_{\text{e1}}^{\parallel} - i \bar{c}_{q\perp}^{\parallel} n_0 v_{\text{te}} T_{\text{e1}}^{\perp} + \bar{c}_{qu}^{\parallel} n_0 T_{\text{e0}} u_{\text{ei1z}}, \quad (\text{B.1})$$

$$q_{\text{e1z}}^{\perp} = -i \bar{c}_{q\parallel}^{\perp} n_0 v_{\text{te}} T_{\text{e1}}^{\parallel} - i \bar{c}_{q\perp}^{\perp} n_0 v_{\text{te}} T_{\text{e1}}^{\perp} + \bar{c}_{qu}^{\perp} n_0 T_{\text{e0}} u_{\text{ei1z}}, \quad (\text{B.2})$$

where 6 dimensionless parameters are defined as

$$\bar{c}_{q\parallel}^{\parallel} = \frac{9}{25}\bar{k}_{\parallel}\bar{K}_{hh} - \frac{8}{5}\bar{k}_{\parallel}\bar{K}_{h\sigma} + \frac{2}{3}\bar{k}_{\parallel}\bar{K}_{\sigma\sigma} - \frac{4}{5}\bar{K}_{hS} - \frac{2}{3}\bar{K}_{\sigma S}, \quad (\text{B.3})$$

$$\bar{c}_{q\perp}^{\parallel} = \frac{6}{25}\bar{k}_{\parallel}\bar{K}_{hh} + \frac{4}{15}\bar{k}_{\parallel}\bar{K}_{h\sigma} - \frac{2}{3}\bar{k}_{\parallel}\bar{K}_{\sigma\sigma} + \frac{4}{5}\bar{K}_{hS} + \frac{2}{3}\bar{K}_{\sigma S}, \quad (\text{B.4})$$

$$\bar{c}_{qu}^{\parallel} = \frac{6}{5}\bar{K}_{hR} + \bar{K}_{\sigma R}, \quad (\text{B.5})$$

$$\bar{c}_{q\parallel}^{\perp} = \frac{3}{25}\bar{k}_{\parallel}\bar{K}_{hh} + \frac{2}{15}\bar{k}_{\parallel}\bar{K}_{h\sigma} - \frac{1}{3}\bar{k}_{\parallel}\bar{K}_{\sigma\sigma} - \frac{4}{15}\bar{K}_{hS} + \frac{1}{3}\bar{K}_{\sigma S}, \quad (\text{B.6})$$

$$\bar{c}_{q\perp}^{\perp} = \frac{2}{25}\bar{k}_{\parallel}\bar{K}_{hh} + \frac{8}{15}\bar{k}_{\parallel}\bar{K}_{h\sigma} + \frac{1}{3}\bar{k}_{\parallel}\bar{K}_{\sigma\sigma} + \frac{4}{15}\bar{K}_{hS} - \frac{1}{3}\bar{K}_{\sigma S}, \quad (\text{B.7})$$

$$\bar{c}_{qu}^{\perp} = \frac{2}{5}\bar{K}_{hR} - \frac{1}{2}\bar{K}_{\sigma R}. \quad (\text{B.8})$$

Here $u_{\text{ei}1z} = u_{\text{e}1z} - u_{\text{i}1z}$ is the the first-order relative flow velocity along the z direction.

With Eqns. 7, 9, 37, 38, 42, and 45, $Q_{\text{e}1}$ can be written as

$$Q_{\text{e}1} = \left(1 - \bar{K}_{RR} + \frac{\alpha^{\parallel}\tau_{\text{ee}}}{\tau_{\text{ei}}} \right) \frac{n_0 m_{\text{e}} u_{\text{e}0z}}{\tau_{\text{ee}}} u_{\text{ei}1z} + \frac{\bar{c}_{Q\parallel} n_0}{\tau_{\text{ee}}} T_{\text{e}1}^{\parallel} + \frac{\bar{c}_{Q\perp} n_0}{\tau_{\text{ee}}} T_{\text{e}1}^{\perp} + A_Q, \quad (\text{B.9})$$

where

$$\bar{c}_{Q\parallel} = -\frac{m_{\text{e}}\tau_{\text{ee}}}{m_{\text{i}}\tau_{\text{ei}}} + \frac{i\bar{k}_{\parallel}u_{\text{e}0z}}{v_{\text{te}}} \left(\frac{3\bar{K}_{hR}}{5} + \frac{\bar{K}_{\sigma R}}{2} - \frac{4\bar{K}_{RS}}{3\bar{k}_{\parallel}} \right) + \frac{i\bar{k}_{\perp}\beta^{\perp}u_{\text{e}0x}}{3v_{\text{te}}}, \quad (\text{B.10})$$

$$\bar{c}_{Q\perp} = -\frac{2m_{\text{e}}\tau_{\text{ee}}}{m_{\text{i}}\tau_{\text{ei}}} + \frac{i\bar{k}_{\parallel}u_{\text{e}0z}}{v_{\text{te}}} \left(\frac{2\bar{K}_{hR}}{5} - \frac{\bar{K}_{\sigma R}}{2} + \frac{4\bar{K}_{RS}}{3\bar{k}_{\parallel}} \right) + \frac{2i\bar{k}_{\perp}\beta^{\perp}u_{\text{e}0x}}{3v_{\text{te}}}, \quad (\text{B.11})$$

$$A_Q = \left[\frac{3m_{\text{e}}(T_{\text{i}0} - T_{\text{e}0})}{m_{\text{i}}\tau_{\text{ei}}} + \frac{\alpha^{\perp}m_{\text{e}}u_{\text{e}0x}^2}{\tau_{\text{ei}}} \right] n_{\text{e}1} + \frac{3m_{\text{e}}n_0}{m_{\text{i}}\tau_{\text{ei}}} T_{\text{i}1} + \frac{2\alpha^{\perp}m_{\text{e}}n_0 \cdot u_{\text{e}0x}}{\tau_{\text{ei}}} u_{\text{ei}1x}. \quad (\text{B.12})$$

With Eqns. 32, 33, 34, and B.9, $C_{\text{e}1}^{\parallel}$ and $C_{\text{e}1}^{\perp}$ can be written as

$$C_{\text{e}1}^{\parallel} = \bar{c}_{C\parallel}^{\parallel} \frac{n_0 T_{\text{e}1}^{\parallel}}{\tau_{\text{ee}}} + \bar{c}_{C\perp}^{\parallel} \frac{n_0 T_{\text{e}1}^{\perp}}{\tau_{\text{ee}}} + \bar{c}_{Cu}^{\parallel} \frac{n_0 T_{\text{e}0} u_{\text{ei}1z}}{\tau_{\text{ee}} v_{\text{te}}} + \frac{2}{3} A_Q, \quad (\text{B.13})$$

$$C_{\text{e}1}^{\perp} = \bar{c}_{C\parallel}^{\perp} \frac{n_0 T_{\text{e}1}^{\parallel}}{\tau_{\text{ee}}} + \bar{c}_{C\perp}^{\perp} \frac{n_0 T_{\text{e}1}^{\perp}}{\tau_{\text{ee}}} + \bar{c}_{Cu}^{\perp} \frac{n_0 T_{\text{e}0} u_{\text{ei}1z}}{\tau_{\text{ee}} v_{\text{te}}} + \frac{2}{3} A_Q, \quad (\text{B.14})$$

where 6 dimensionless parameters are given by

$$\bar{c}_{C\parallel}^{\parallel} = \frac{2}{3}\bar{c}_{Q\parallel} + \frac{4}{5}\bar{k}_{\parallel}\bar{K}_{hS} + \frac{2}{3}\bar{k}_{\parallel}\bar{K}_{\sigma S} - \frac{2(2.05 - \bar{K}_{SS})}{3}, \quad (\text{B.15})$$

$$\bar{c}_{C\perp}^{\parallel} = \frac{2}{3}\bar{c}_{Q\perp} + \frac{8}{15}\bar{k}_{\parallel}\bar{K}_{hS} - \frac{2}{3}\bar{k}_{\parallel}\bar{K}_{\sigma S} + \frac{2(2.05 - \bar{K}_{SS})}{3}, \quad (\text{B.16})$$

$$\bar{c}_{Cu}^{\parallel} = \frac{4}{3} \left(1 - \bar{K}_{RR} + \frac{\alpha^{\parallel} \tau_{ee}}{\tau_{ei}} \right) \frac{u_{e0z}}{v_{te}} + \frac{8i}{3} \bar{K}_{RS}, \quad (B.17)$$

$$\bar{c}_{C\parallel}^{\perp} = \frac{2}{3} \bar{c}_{Q\parallel} - \frac{2}{5} \bar{k}_{\parallel} \bar{K}_{hS} - \frac{1}{3} \bar{k}_{\parallel} \bar{K}_{\sigma S} + \frac{2.05 - \bar{K}_{SS}}{3}, \quad (B.18)$$

$$\bar{c}_{C\perp}^{\perp} = \frac{2}{3} \bar{c}_{Q\perp} - \frac{4}{15} \bar{k}_{\parallel} \bar{K}_{hS} + \frac{1}{3} \bar{k}_{\parallel} \bar{K}_{\sigma S} - \frac{2.05 - \bar{K}_{SS}}{3}, \quad (B.19)$$

$$\bar{c}_{Cu}^{\perp} = \frac{4}{3} \left(1 - \bar{K}_{RR} + \frac{\alpha^{\parallel} \tau_{ee}}{\tau_{ei}} \right) \frac{u_{e0z}}{v_{te}} - \frac{4i}{3} \bar{K}_{RS}. \quad (B.20)$$

With these closures, Eqns. 20 and 21 can be written as

$$ir\alpha_e T_{e1}^{\parallel} = \bar{c}_{\parallel}^{\parallel} T_{e1}^{\parallel} + \bar{c}_{\perp}^{\parallel} T_{e1}^{\perp} + \bar{c}_u^{\parallel} T_{e0} \frac{u_{e1z}}{v_{te}} - \bar{c}_{ux} T_{e0} \frac{u_{e1x}}{v_{te}} - \bar{c}_n T_{e0} \frac{n_{e1}}{n_0} + A_t^{\parallel}, \quad (B.21)$$

$$ir\alpha_e T_{e1}^{\perp} = \bar{c}_{\parallel}^{\perp} T_{e1}^{\parallel} + \bar{c}_{\perp}^{\perp} T_{e1}^{\perp} + \bar{c}_u^{\perp} T_{e0} \frac{u_{e1z}}{v_{te}} + (i\bar{k}_{\perp} - \bar{c}_{ux}) T_{e0} \frac{u_{e1x}}{v_{te}} - \bar{c}_n T_{e0} \frac{n_{e1}}{n_0} + A_t^{\perp}, \quad (B.22)$$

where

$$\alpha_e = (\omega - \mathbf{k} \cdot \mathbf{u}_{e0})/\omega_{ce}, \quad (B.23)$$

$$\bar{c}_{\parallel}^{\parallel} = \bar{k}_{\parallel} \bar{c}_{q\parallel}^{\parallel} - \bar{c}_{C\parallel}^{\parallel} + ir_{te} k_{\perp} \tau_{ee} u_{e0x}, \quad (B.24)$$

$$\bar{c}_{\perp}^{\parallel} = \bar{k}_{\parallel} \bar{c}_{q\perp}^{\parallel} - \bar{c}_{C\perp}^{\parallel} - ir_{te} k_{\perp} \tau_{ee} u_{e0x}, \quad (B.25)$$

$$\bar{c}_u^{\parallel} = i\bar{k}_{\parallel} \bar{c}_{qu}^{\parallel} - \bar{c}_{Cu}^{\parallel} + 2i\bar{k}_{\parallel}, \quad (B.26)$$

$$\bar{c}_{ux} = \frac{8\alpha^{\perp} \tau_{ee} u_{e0x}}{3\tau_{ei} v_{te}} \quad (B.27)$$

$$\bar{c}_n = \frac{2m_e \tau_{ee}}{m_i \tau_{ei}} \left(\frac{T_{i0}}{T_{e0}} - 1 \right) + \frac{4\alpha^{\perp} \tau_{ee} u_{e0x}^2}{3\tau_{ei} v_{te}^2} \quad (B.28)$$

$$\bar{c}_{\parallel}^{\perp} = \bar{k}_{\parallel} \bar{c}_{q\parallel}^{\perp} - \bar{c}_{C\parallel}^{\perp} - ir_{te} k_{\perp} \tau_{ee} u_{e0x}, \quad (B.29)$$

$$\bar{c}_{\perp}^{\perp} = \bar{k}_{\parallel} \bar{c}_{q\perp}^{\perp} - \bar{c}_{C\perp}^{\perp} + ir_{te} k_{\perp} \tau_{ee} u_{e0x}, \quad (B.30)$$

$$\bar{c}_u^{\perp} = i\bar{k}_{\parallel} \bar{c}_{qu}^{\perp} - \bar{c}_{Cu}^{\perp}, \quad (B.31)$$

$$A_t^{\parallel} = -\frac{2m_e \tau_{ee}}{m_i \tau_{ei}} T_{i1} - \left(i\bar{k}_{\parallel} \bar{c}_{qu}^{\parallel} - \bar{c}_{Cu}^{\parallel} \right) T_{e0} \frac{u_{i1z}}{v_{te}} + \frac{8\alpha^{\perp} \tau_{ee} u_{e0x}}{3\tau_{ei} v_{te}} T_{e0} \frac{u_{i1x}}{v_{te}}, \quad (B.32)$$

$$A_t^{\perp} = -\frac{2m_e \tau_{ee}}{m_i \tau_{ei}} T_{i1} - \left(i\bar{k}_{\parallel} \bar{c}_{qu}^{\perp} - \bar{c}_{Cu}^{\perp} \right) T_{e0} \frac{u_{i1z}}{v_{te}} + \frac{8\alpha^{\perp} \tau_{ee} u_{e0x}}{3\tau_{ei} v_{te}} T_{e0} \frac{u_{i1x}}{v_{te}}. \quad (B.33)$$

With Eqns. B.21 and B.22, the T_{e1}^{\parallel} and T_{e1}^{\perp} can be written as

$$T_{e1}^{\parallel} = \bar{c}_{uz}^{\parallel} T_{e0} \frac{u_{e1z}}{v_{te}} + \bar{c}_{ux}^{\parallel} T_{e0} \frac{u_{e1x}}{v_{te}} + \bar{c}_n^{\parallel} T_{e0} \frac{n_{e1}}{n_0} + A_i^{\parallel}, \quad (B.34)$$

Collisional effects on lower hybrid drift waves

$$T_{e1}^{\perp} = \bar{c}_{uz}^{\perp} T_{e0} \frac{u_{e1z}}{v_{te}} + \bar{c}_{ux}^{\perp} T_{e0} \frac{u_{e1x}}{v_{te}} + \bar{c}_n^{\perp} T_{e0} \frac{n_{e1}}{n_0} + A_i^{\perp}, \quad (B.35)$$

where

$$\bar{c}_{uz}^{\parallel} = \frac{(ir\alpha_e - \bar{c}_{\perp}^{\perp}) \bar{c}_u^{\parallel} + \bar{c}_{\perp}^{\parallel} \bar{c}_u^{\perp}}{(ir\alpha_e - \bar{c}_{\parallel}^{\parallel}) (ir\alpha_e - \bar{c}_{\perp}^{\perp}) - \bar{c}_{\perp}^{\parallel} \bar{c}_{\parallel}^{\perp}}, \quad (B.36)$$

$$\bar{c}_{ux}^{\parallel} = -\frac{(ir\alpha_e - \bar{c}_{\perp}^{\perp}) \bar{c}_{ux} - \bar{c}_{\perp}^{\parallel} (i\bar{k}_{\perp} - \bar{c}_{ux})}{(ir\alpha_e - \bar{c}_{\parallel}^{\parallel}) (ir\alpha_e - \bar{c}_{\perp}^{\perp}) - \bar{c}_{\perp}^{\parallel} \bar{c}_{\parallel}^{\perp}}, \quad (B.37)$$

$$\bar{c}_n^{\parallel} = -\frac{(ir\alpha_e - \bar{c}_{\perp}^{\perp} + \bar{c}_{\perp}^{\parallel}) \bar{c}_n}{(ir\alpha_e - \bar{c}_{\parallel}^{\parallel}) (ir\alpha_e - \bar{c}_{\perp}^{\perp}) - \bar{c}_{\perp}^{\parallel} \bar{c}_{\parallel}^{\perp}}, \quad (B.38)$$

$$\bar{c}_{uz}^{\perp} = \frac{(ir\alpha_e - \bar{c}_{\parallel}^{\parallel}) \bar{c}_u^{\perp} + \bar{c}_{\parallel}^{\perp} \bar{c}_u^{\parallel}}{(ir\alpha_e - \bar{c}_{\parallel}^{\parallel}) (ir\alpha_e - \bar{c}_{\perp}^{\perp}) - \bar{c}_{\perp}^{\parallel} \bar{c}_{\parallel}^{\perp}}, \quad (B.39)$$

$$\bar{c}_{ux}^{\perp} = \frac{(ir\alpha_e - \bar{c}_{\parallel}^{\parallel}) (i\bar{k}_{\perp} - \bar{c}_{ux}) - \bar{c}_{\parallel}^{\perp} \bar{c}_{ux}}{(ir\alpha_e - \bar{c}_{\parallel}^{\parallel}) (ir\alpha_e - \bar{c}_{\perp}^{\perp}) - \bar{c}_{\perp}^{\parallel} \bar{c}_{\parallel}^{\perp}}, \quad (B.40)$$

$$\bar{c}_n^{\perp} = -\frac{(ir\alpha_e - \bar{c}_{\parallel}^{\parallel} + \bar{c}_{\parallel}^{\perp}) \bar{c}_n}{(ir\alpha_e - \bar{c}_{\parallel}^{\parallel}) (ir\alpha_e - \bar{c}_{\perp}^{\perp}) - \bar{c}_{\perp}^{\parallel} \bar{c}_{\parallel}^{\perp}}. \quad (B.41)$$

The additional ion terms A_i^{\parallel} and A_i^{\perp} can be expressed as

$$A_i^{\parallel} = \bar{c}_{i\parallel}^{\parallel} A_t^{\parallel} + \bar{c}_{i\perp}^{\parallel} A_t^{\perp}, \quad (B.42)$$

$$A_i^{\perp} = \bar{c}_{i\parallel}^{\perp} A_t^{\parallel} + \bar{c}_{i\perp}^{\perp} A_t^{\perp}, \quad (B.43)$$

where

$$\bar{c}_{i\parallel}^{\parallel} = \frac{ir\alpha_e - \bar{c}_{\perp}^{\perp}}{(ir\alpha_e - \bar{c}_{\parallel}^{\parallel}) (ir\alpha_e - \bar{c}_{\perp}^{\perp}) - \bar{c}_{\perp}^{\parallel} \bar{c}_{\parallel}^{\perp}}, \quad (B.44)$$

$$\bar{c}_{i\perp}^{\parallel} = \frac{\bar{c}_{\perp}^{\parallel}}{(ir\alpha_e - \bar{c}_{\parallel}^{\parallel}) (ir\alpha_e - \bar{c}_{\perp}^{\perp}) - \bar{c}_{\perp}^{\parallel} \bar{c}_{\parallel}^{\perp}}, \quad (B.45)$$

$$\bar{c}_{i\parallel}^{\perp} = \frac{\bar{c}_{\parallel}^{\perp}}{(ir\alpha_e - \bar{c}_{\parallel}^{\parallel}) (ir\alpha_e - \bar{c}_{\perp}^{\perp}) - \bar{c}_{\perp}^{\parallel} \bar{c}_{\parallel}^{\perp}}, \quad (B.46)$$

$$\bar{c}_{i\perp}^{\perp} = \frac{ir\alpha_e - \bar{c}_{\parallel}^{\parallel}}{(ir\alpha_e - \bar{c}_{\parallel}^{\parallel}) (ir\alpha_e - \bar{c}_{\perp}^{\perp}) - \bar{c}_{\perp}^{\parallel} \bar{c}_{\parallel}^{\perp}}. \quad (B.47)$$

The z component of Eqn. 8 is

$$im_en_0(\omega - \mathbf{k} \cdot \mathbf{u}_0)u_{e1z} = ik_{\parallel}p_{e1}^{\parallel} + en_0(E_{1z} + u_{0x}B_{1y}) - R_{e1}^{\parallel}. \quad (\text{B.48})$$

From the Faraday's Law ($\omega\mathbf{B}_1 = \mathbf{k} \times \mathbf{E}_1$), $B_{1y} = (k_{\parallel}E_{1x} - k_{\perp}E_{1z})/\omega$. With Eqns. 9, B.34, B.35, B.48, and 42, u_{e1z} is expressed as

$$i\alpha_{ez}u_{e1z} = i\bar{c}_{xz}u_{e1x} + \bar{c}_{yz}u_{e1y} + A_{ez} + A_{iz}, \quad (\text{B.49})$$

where

$$\alpha_{ez} = \alpha_e - \frac{k_{\parallel}v_{te}}{2\omega_{ce}} \left[\bar{c}_{uz}^{\parallel} + \gamma_{ez}^{\parallel}\bar{c}_{uz}^{\parallel} + \gamma_{ez}^{\perp}\bar{c}_{uz}^{\perp} - \frac{2i(1 - \bar{K}_{RR})}{\bar{k}_{\parallel}} + \frac{k_{\parallel}v_{te}}{\alpha_e\omega_{ce}} \left(1 + \bar{c}_n^{\parallel} + \gamma_{ez}^{\parallel}\bar{c}_n^{\parallel} + \gamma_{ez}^{\perp}\bar{c}_n^{\perp} \right) \right], \quad (\text{B.50})$$

$$\bar{c}_{xz} = \frac{k_{\parallel}v_{te}}{2\omega_{ce}} \left[\bar{c}_{ux}^{\parallel} + \gamma_{ez}^{\parallel}\bar{c}_{ux}^{\parallel} + \gamma_{ez}^{\perp}\bar{c}_{ux}^{\perp} + \frac{k_{\perp}v_{te}}{\alpha_e\omega_{ce}} \left(1 + \bar{c}_n^{\parallel} + \gamma_{ez}^{\parallel}\bar{c}_n^{\parallel} + \gamma_{ez}^{\perp}\bar{c}_n^{\perp} \right) \right], \quad (\text{B.51})$$

$$\bar{c}_{yz} = \frac{\epsilon k_{\parallel}v_{te}^2}{2\alpha_e\omega_{ce}^2} \left(1 + \bar{c}_n^{\parallel} + \gamma_{ez}^{\parallel}\bar{c}_n^{\parallel} + \gamma_{ez}^{\perp}\bar{c}_n^{\perp} \right), \quad (\text{B.52})$$

$$A_{ez} = \frac{E_{1z}}{B_0} + \frac{ku_{0x}}{\omega} \frac{E_{1x}\cos\theta - E_{1z}\sin\theta}{B_0}, \quad (\text{B.53})$$

$$A_{iz} = \frac{ik_{\parallel}}{eB_0} \left(A_i^{\parallel} + \gamma_{ez}^{\parallel}A_i^{\parallel} + \gamma_{ez}^{\perp}A_i^{\perp} \right) - \frac{1 - \bar{K}_{RR}}{\omega_{ce}\tau_{ee}}u_{i1z}. \quad (\text{B.54})$$

The x component of Eqn. 8 is

$$im_en_0(\omega - \mathbf{k} \cdot \mathbf{u}_{e0})u_{e1x} = ik_{\perp}(n_0T_{e1}^{\perp} + T_{e0}n_{e1}) + en_0(E_{1x} + B_0u_{e1y} - u_{e0z}B_{1y}) - R_{e1}^{\perp}. \quad (\text{B.55})$$

With Eqns. 9, B.34, B.35, 45, B.49, and B.55, u_{e1y} can be expressed as

$$\gamma_{ey}u_{e1y} = i\alpha_{ex}u_{e1x} - A_{ex} - A_{ix} - \frac{\bar{c}_{zx}k_{\perp}v_{te}}{2\alpha_{ez}\omega_{ce}}(A_{ez} + A_{iz}), \quad (\text{B.56})$$

where γ_{ey} , α_{ex} , and A_{ex} are

$$\gamma_{ey} = 1 + \frac{\bar{c}_{nx}\epsilon k_{\perp}v_{te}^2}{2\alpha_e\omega_{ce}^2} + \frac{\bar{c}_{zx}\bar{c}_{yz}k_{\perp}v_{te}}{2\alpha_{ez}\omega_{ce}}, \quad (\text{B.57})$$

$$\alpha_{ex} = \alpha_e - \frac{\bar{c}_{nx}k_{\perp}^2v_{te}^2}{2\alpha_e\omega_{ce}^2} - \frac{\bar{c}_{zx}\bar{c}_{xz}k_{\perp}v_{te}}{2\alpha_{ez}\omega_{ce}} - \frac{k_{\perp}v_{te}}{2\omega_{ce}} \left[\frac{\beta^{\perp}\bar{c}_{ux}^{\parallel}}{3} + \left(1 + \frac{2\beta^{\perp}}{3} \right) \bar{c}_{ux}^{\perp} - \frac{2i\alpha^{\perp}\tau_{ee}}{\bar{k}_{\perp}\tau_{ei}} \right], \quad (\text{B.58})$$

$$A_{ex} = \frac{E_{1x}}{B_0} - \frac{ku_{0z}}{\omega} \frac{E_{1x}\cos\theta - E_{1z}\sin\theta}{B_0}, \quad (\text{B.59})$$

$$A_{ix} = \frac{ik_{\perp}}{eB_0} \left[\frac{\beta^{\perp}A_i^{\parallel}}{3} + \left(1 + \frac{2\beta^{\perp}}{3} \right) A_i^{\perp} \right] - \frac{\alpha^{\perp}u_{i1x}}{\tau_{ei}\omega_{ce}}. \quad (\text{B.60})$$

Collisional effects on lower hybrid drift waves

Here two dimensionless parameters are given by

$$\bar{c}_{nx} = 1 + \frac{\beta^\perp \bar{c}_n^\parallel}{3} + \left(1 + \frac{2\beta^\perp}{3}\right) \bar{c}_n^\perp - \frac{2i\alpha^\perp \tau_{ee} u_{e0x}}{\bar{k}_\perp \tau_{ei} v_{te}}, \quad (\text{B.61})$$

$$\bar{c}_{zx} = \frac{\beta^\perp \bar{c}_{uz}^\parallel}{3} + \left(1 + \frac{2\beta^\perp}{3}\right) \bar{c}_{uz}^\perp + \frac{\bar{c}_{nx} k_\parallel v_{te}}{\alpha_e \omega_{ce}}. \quad (\text{B.62})$$

Similarly, the y component of Eqn. 8 is

$$im_e n_0 (\omega - \mathbf{k} \cdot \mathbf{u}_0) u_{e1y} = en_0 (E_{1y} - B_0 u_{e1x} - u_{e0x} B_{1z} + u_{e0z} B_{1x}) + e(E_0 - u_{e0x} B_0) n_{e1} - R_{e1}^\times. \quad (\text{B.63})$$

With Eqns. 9, 3, and B.49, u_{e1x} can be expressed as

$$\gamma_{ex} u_{e1x} = -i\alpha_{ey} u_{e1y} + \frac{3ir_{te} k_\parallel u_{0x}}{2\alpha_e \alpha_{ez} \omega_{ce}} (A_{ez} + A_{iz}) + A_{ey} + A_{iy}, \quad (\text{B.64})$$

where γ_{ex} , α_{ey} , A_{ey} , and A_{iy} are

$$\gamma_{ex} = 1 + \frac{3r_{te} k_\perp u_{e0x}}{2\alpha_e \omega_{ce}} \left(1 + \frac{\bar{c}_{xz} k_\parallel}{\alpha_{ez} k_\perp}\right), \quad (\text{B.65})$$

$$\alpha_{ey} = \alpha_e - i \frac{\alpha^\times}{\omega_{ce} \tau_{ei}} - \frac{3r_{te} \epsilon u_{e0x}}{2\alpha_e \omega_{ce}} \left(1 + \frac{\bar{c}_{yz} k_\parallel}{\alpha_{ez} \epsilon}\right), \quad (\text{B.66})$$

$$A_{ey} = \frac{E_{1y}}{B_0} - \frac{k}{\omega} \frac{(u_{0x} \sin \theta + u_{0z} \cos \theta) E_{1y}}{B_0}, \quad (\text{B.67})$$

$$A_{iy} = \frac{\alpha^\times}{\omega_{ce} \tau_{ei}} u_{i1y}. \quad (\text{B.68})$$

With Eqns. B.56 and B.64, u_{e1y} is given by

$$u_{e1y} = i [iC_{yx}^e (A_{ex} + A_{ix}) + C_{yy}^e (A_{ey} + A_{iy}) + iC_{yz}^e (A_{ez} + A_{iz})], \quad (\text{B.69})$$

where

$$C_{yx}^e = \left(\gamma_{ey} - \frac{\alpha_{ex} \alpha_{ey}}{\gamma_{ex}} \right)^{-1}, \quad (\text{B.70})$$

$$C_{yy}^e = C_{yx}^e \frac{\alpha_{ex}}{\gamma_{ex}}, \quad (\text{B.71})$$

$$C_{yz}^e = C_{yx}^e \left(\frac{\bar{c}_{zx} k_\perp v_{te}}{2\alpha_{ez} \omega_{ce}} + \frac{3r_{te} \alpha_{ex} k_\parallel u_{e0x}}{2\gamma_{ex} \alpha_e \alpha_{ez} \omega_{ce}} \right). \quad (\text{B.72})$$

Similarly, u_{e1x} is given by

$$u_{e1x} = iC_{xx}^e (A_{ex} + A_{ix}) + C_{xy}^e (A_{ey} + A_{iy}) + iC_{xz}^e (A_{ez} + A_{iz}), \quad (\text{B.73})$$

where

$$C_{xy}^e = \left(\gamma_{ex} - \frac{\alpha_{ex}\alpha_{ey}}{\gamma_{ey}} \right)^{-1}, \quad (B.74)$$

$$C_{xx}^e = C_{xy}^e \frac{\alpha_{ey}}{\gamma_{ey}}, \quad (B.75)$$

$$C_{xz}^e = C_{xy}^e \left[\frac{3r_{te}k_{\parallel}u_{0x}}{2\alpha_e\alpha_{ez}\omega_{ce}} + \frac{\alpha_{ey}\bar{c}_{zx}k_{\perp}v_{te}}{2\gamma_{ey}\alpha_{ez}\omega_{ce}} \right]. \quad (B.76)$$

Then, u_{e1z} can be written as

$$u_{e1z} = iC_{zx}^e(A_{ex} + A_{ix}) + C_{zy}^e(A_{ey} + A_{iy}) + iC_{zz}^e(A_{ez} + A_{iz}), \quad (B.77)$$

where

$$C_{zz}^e = -\frac{1}{\alpha_{ez}} + \frac{\bar{c}_{xz}C_{xz}^e}{\alpha_{ez}} + \frac{\bar{c}_{yz}C_{yz}^e}{\alpha_{ez}}, \quad (B.78)$$

$$C_{zx}^e = \frac{\bar{c}_{xz}C_{xx}^e}{\alpha_{ez}} + \frac{\bar{c}_{yz}C_{yx}^e}{\alpha_{ez}}, \quad (B.79)$$

$$C_{zy}^e = \frac{\bar{c}_{xz}C_{xy}^e}{\alpha_{ez}} + \frac{\bar{c}_{yz}C_{yy}^e}{\alpha_{ez}}. \quad (B.80)$$

The final goal is to obtain the perturbed current density of electrons, which is given by $\mathbf{J}_1^e = -en_0\mathbf{u}_{e1} - e\mathbf{u}_{e0}n_{e1}$. Thus, an expression for n_{e1} is required. From Eqns. 9, B.69, B.73, and B.77, n_{e1} is given by

$$n_{e1} = \frac{kn_0}{\omega - \mathbf{k} \cdot \mathbf{u}_{e0}} [iC'_x^e(A_{ex} + A_{ix}) + C'_y^e(A_{ey} + A_{iy}) + iC'_z^e(A_{ez} + A_{iz})], \quad (B.81)$$

where

$$C'_x^e = C_{xx}^e \sin \theta + C_{yx}^e \mathcal{E}/k + C_{zx}^e \cos \theta, \quad (B.82)$$

$$C'_y^e = C_{xy}^e \sin \theta + C_{yy}^e \mathcal{E}/k + C_{zy}^e \cos \theta, \quad (B.83)$$

$$C'_z^e = C_{xz}^e \sin \theta + C_{yz}^e \mathcal{E}/k + C_{zz}^e \cos \theta. \quad (B.84)$$

Now we are ready for computing the dispersion relation. Eqn. 5 is

$$k_{\parallel}^2 E_{1x} - k_{\perp} k_{\parallel} E_{1z} - i\omega \mu_0 J_{1x} = 0, \quad (B.85)$$

$$k^2 E_{1y} - i\omega \mu_0 J_{1y} = 0, \quad (B.86)$$

$$k_{\perp}^2 E_{1z} - k_{\perp} k_{\parallel} E_{1x} - i\omega \mu_0 J_{1z} = 0. \quad (B.87)$$

Collisional effects on lower hybrid drift waves

By multiplying by d_i^2 ($d_i \equiv c/\omega_{pi}$ is the ion skin depth; ω_{pi} is ion plasma frequency), the above equation can be written as

$$K^2 \cos^2 \theta E_{1x} - K^2 \sin \theta \cos \theta E_{1z} - i\Omega \frac{B_0}{en_0} J_{1x} = 0, \quad (\text{B.88})$$

$$K^2 E_{1y} - i\Omega \frac{B_0}{en_0} J_{1y} = 0, \quad (\text{B.89})$$

$$K^2 \sin^2 \theta E_{1z} - K^2 \sin \theta \cos \theta E_{1x} - i\Omega \frac{B_0}{en_0} J_{1z} = 0, \quad (\text{B.90})$$

where $K \equiv kd_i$ and $\Omega = \omega/\omega_{ci}$.

From Eqn. 6, each component of $i\Omega B_0 \mathbf{J}_1^i / en_0$ is

$$\frac{i\Omega B_0}{en_0} J_{1x}^i = \zeta Z E_{1x} + \frac{\zeta Z'' \sin \theta}{2} \left(E_{1x} \sin \theta - i\frac{\epsilon}{k} E_{1y} + E_{1z} \cos \theta \right), \quad (\text{B.91})$$

$$\frac{i\Omega B_0}{en_0} J_{1y}^i = \zeta Z E_{1y}, \quad (\text{B.92})$$

$$\frac{i\Omega B_0}{en_0} J_{1z}^i = \zeta Z E_{1z} + \frac{\zeta Z'' \cos \theta}{2} \left(E_{1x} \sin \theta - i\frac{\epsilon}{k} E_{1y} + E_{1z} \cos \theta \right). \quad (\text{B.93})$$

From Eqns. B.73 and B.81, iJ_{1x}^e / en_0 is given by

$$\frac{iJ_{1x}^e}{en_0} = C_{xx}^e (A_{ex} + A_{ix}) - iC_{xy}^e (A_{ey} + A_{iy}) + C_{xz}^e (A_{ez} + A_{iz}), \quad (\text{B.94})$$

where $C_{xx}^e = C_{xx} + ku_{e0x} C_x'^e / (\omega - \mathbf{k} \cdot \mathbf{u}_{e0})$, $C_{xy}^e = C_{xy} + ku_{e0x} C_y'^e / (\omega - \mathbf{k} \cdot \mathbf{u}_{e0})$, and $C_{xz}^e = C_{xz} + ku_{e0x} C_z'^e / (\omega - \mathbf{k} \cdot \mathbf{u}_{e0})$. Similarly, from Eqns. B.77 and B.81, iJ_{1z}^e / en_0 is given by

$$\frac{iJ_{1z}^e}{en_0} = C_{zx}^e (A_{ex} + A_{ix}) - iC_{zy}^e (A_{ey} + A_{iy}) + C_{zz}^e (A_{ez} + A_{iz}), \quad (\text{B.95})$$

where $C_{zx}^e = C_{zx} + ku_{e0z} C_x'^e / (\omega - \mathbf{k} \cdot \mathbf{u}_{e0})$, $C_{zy}^e = C_{zy} + ku_{e0z} C_y'^e / (\omega - \mathbf{k} \cdot \mathbf{u}_{e0})$, and $C_{zz}^e = C_{zz} + ku_{e0z} C_z'^e / (\omega - \mathbf{k} \cdot \mathbf{u}_{e0})$. Since there is no y component in \mathbf{u}_{e0} , iJ_{1y}^e / en_0 is simply

$$\frac{iJ_{1y}^e}{en_0} = iC_{yx}^e (A_{ex} + A_{ix}) + C_{yy}^e (A_{ey} + A_{iy}) + iC_{yz}^e (A_{ez} + A_{iz}). \quad (\text{B.96})$$

In terms of dimensionless parameters, $\Omega B_0 A_{ex}$, $\Omega B_0 A_{ey}$, and $\Omega B_0 A_{ez}$ can be written as

$$\Omega B_0 A_{ex} = (\Omega - K U_{e0z} \cos \theta) E_{1x} + (K U_{e0z} \sin \theta) E_{1z}, \quad (\text{B.97})$$

$$\Omega B_0 A_{ey} = [\Omega - K (U_{e0x} \sin \theta + U_{e0z} \cos \theta)] E_{1y}, \quad (\text{B.98})$$

$$\Omega B_0 A_{ez} = (K U_{e0x} \cos \theta) E_{1x} + (\Omega - K U_{e0x} \sin \theta) E_{1z}, \quad (\text{B.99})$$

$\mathbf{U}_{e0} = \mathbf{u}_{e0}/V_A$ and $V_A = B_0/\sqrt{\mu_0 m_i n_0} = d_i \omega_{ci}$ is the Alfvén speed.

With Eqn. 7, A_{iz} in Eqn. B.54 is

$$A_{iz} = \bar{c}_{izx} \frac{iJ_{1x}^i}{en_0} + \bar{c}_{izz} \frac{iJ_{1z}^i}{en_0} + \frac{\bar{c}_{izT}}{B_0} \left[\mathbf{E}_1 \cdot \hat{\mathbf{k}} \left(2Z' + \frac{Z'''}{4} \right) - iE_{1y} \left(\frac{\epsilon}{k} \right) \left(Z' + \frac{Z'''}{4} \right) \right], \quad (\text{B.100})$$

where three dimensionless parameters are given by

$$\bar{c}_{izx} = \frac{4\alpha^\perp (\bar{c}_{iz}^\parallel + \bar{c}_{iz}^\perp) \tau_{ee} k_\parallel u_{e0x}}{3\tau_{ei} \omega_{ce}}, \quad (\text{B.101})$$

$$\bar{c}_{izz} = - \left[\bar{c}_{iz}^\parallel \left(i\bar{k}_\parallel \bar{c}_{qu}^\parallel - \bar{c}_{Cu}^\parallel \right) + \bar{c}_{iz}^\perp \left(i\bar{k}_\parallel \bar{c}_{qu}^\perp - \bar{c}_{Cu}^\perp \right) \right] \frac{k_\parallel v_{te}}{2\omega_{ce}} + \frac{i(1 - \bar{K}_{RR})}{\omega_{ce} \tau_{ee}}, \quad (\text{B.102})$$

$$\bar{c}_{izT} = \frac{2(\bar{c}_{iz}^\parallel + \bar{c}_{iz}^\perp) m_e \tau_{ee} \cos \theta}{m_i \tau_{ei}}. \quad (\text{B.103})$$

Here two additional parameters \bar{c}_{iz}^\parallel and \bar{c}_{iz}^\perp are defined as

$$\bar{c}_{iz}^\parallel = (1 + \gamma_{ez}^\parallel) \bar{c}_{i\parallel}^\parallel + \gamma_{ez}^\perp \bar{c}_{i\parallel}^\perp, \quad (\text{B.104})$$

$$\bar{c}_{iz}^\perp = (1 + \gamma_{ez}^\parallel) \bar{c}_{i\perp}^\parallel + \gamma_{ez}^\perp \bar{c}_{i\perp}^\perp. \quad (\text{B.105})$$

Similarly, A_{ix} is

$$A_{ix} = \bar{c}_{ixx} \frac{iJ_{1x}^i}{en_0} + \bar{c}_{ixz} \frac{iJ_{1z}^i}{en_0} + \frac{\bar{c}_{ixT}}{B_0} \left[\mathbf{E}_1 \cdot \hat{\mathbf{k}} \left(2Z' + \frac{Z'''}{4} \right) - iE_{1y} \left(\frac{\epsilon}{k} \right) \left(Z' + \frac{Z'''}{4} \right) \right], \quad (\text{B.106})$$

where three dimensionless parameters are given by

$$\bar{c}_{ixx} = \frac{4\alpha^\perp (\bar{c}_{ix}^\parallel + \bar{c}_{ix}^\perp) \tau_{ee} k_\perp u_{e0x}}{3\tau_{ei} \omega_{ce}} - \frac{\alpha^\perp}{\tau_{ee} \omega_{ce}}, \quad (\text{B.107})$$

$$\bar{c}_{ixz} = - \left[\bar{c}_{ix}^\parallel \left(i\bar{k}_\parallel \bar{c}_{qu}^\parallel - \bar{c}_{Cu}^\parallel \right) + \bar{c}_{ix}^\perp \left(i\bar{k}_\parallel \bar{c}_{qu}^\perp - \bar{c}_{Cu}^\perp \right) \right] \frac{k_\perp v_{te}}{2\omega_{ce}}, \quad (\text{B.108})$$

$$\bar{c}_{ixT} = \frac{2(\bar{c}_{ix}^\parallel + \bar{c}_{ix}^\perp) m_e \tau_{ee} \sin \theta}{m_i \tau_{ei}}. \quad (\text{B.109})$$

Two additional parameters \bar{c}_{ix}^\parallel and \bar{c}_{ix}^\perp are

$$\bar{c}_{ix}^\parallel = \frac{\beta^\perp}{3} \bar{c}_{i\parallel}^\parallel + \left(1 + \frac{2\beta^\perp}{3} \right) \bar{c}_{i\parallel}^\perp, \quad (\text{B.110})$$

$$\bar{c}_{ix}^\perp = \frac{\beta^\perp}{3} \bar{c}_{i\perp}^\parallel + \left(1 + \frac{2\beta^\perp}{3} \right) \bar{c}_{i\perp}^\perp. \quad (\text{B.111})$$

The last ion term is $A_{iy} = (\alpha^\times / \omega_{ce} \tau_{ei}) J_{1y}^i / en_0$.

Eqns. B.88–B.90 can be written as

$$\begin{pmatrix} D_{xx} & D_{xy} & D_{xz} \\ D_{yx} & D_{yy} & D_{yz} \\ D_{zx} & D_{zy} & D_{zz} \end{pmatrix} \begin{pmatrix} E_{1x} \\ E_{1y} \\ E_{1z} \end{pmatrix} = 0. \quad (\text{B.112})$$

Each component of the tensor \mathbf{D} is

$$D_{xx} = K^2 \cos^2 \theta - C_{xx}' (\Omega - KU_{e0z} \cos \theta) - C_{xz}' KU_{e0x} \cos \theta \quad (\text{B.113})$$

$$- C_{xx}^i \left(\zeta Z + \frac{\zeta Z'' \sin^2 \theta}{2} \right) - C_{xz}^i \frac{\zeta Z'' \cos \theta \sin \theta}{2} - C_{xT}^i \Omega \sin \theta \left(2Z' + \frac{Z'''}{4} \right),$$

$$D_{xy} = C_{xy}' \frac{\alpha^\times}{\omega_{ce} \tau_{ei}} \zeta Z + i C_{xy}' [\Omega - K(U_{e0x} \sin \theta + U_{e0z} \cos \theta)] \quad (\text{B.114})$$

$$+ i \left(\frac{\epsilon}{k} \right) C_{xx}^i \frac{\zeta Z'' \sin \theta}{2} + i \left(\frac{\epsilon}{k} \right) C_{xz}^i \frac{\zeta Z'' \cos \theta}{2} + i \left(\frac{\epsilon}{k} \right) C_{xT}^i \left(Z' + \frac{Z'''}{4} \right),$$

$$D_{xz} = -K^2 \sin \theta \cos \theta - C_{xx}' KU_{e0z} \sin \theta - C_{xz}' (\Omega - KU_{e0x} \sin \theta) \quad (\text{B.115})$$

$$- C_{xx}^i \frac{\zeta Z''}{2} \sin \theta \cos \theta - C_{xz}^i \left(\zeta Z + \frac{\zeta Z'' \cos^2 \theta}{2} \right) - C_{xT}^i \Omega \cos \theta \left(2Z' + \frac{Z'''}{4} \right),$$

$$D_{yx} = -i [C_{yx}^e (\Omega - KU_{e0z} \cos \theta) + C_{yz}^e KU_{e0x} \cos \theta] \quad (\text{B.116})$$

$$- i C_{yx}^i \left(\zeta Z + \frac{\zeta Z'' \sin^2 \theta}{2} \right) - i C_{yz}^i \frac{\zeta Z'' \cos \theta \sin \theta}{2} - i C_{yT}^i \Omega \sin \theta \left(2Z' + \frac{Z'''}{4} \right),$$

$$D_{yy} = K^2 - \left(1 - \frac{i C_{yy}^e \alpha^\times}{\omega_{ce} \tau_{ei}} \right) \zeta Z - C_{yy}^e [\Omega - K(U_{e0x} \sin \theta + U_{e0z} \cos \theta)] \quad (\text{B.117})$$

$$- \left(\frac{\epsilon}{k} \right) C_{yx}^i \frac{\zeta Z'' \sin \theta}{2} - \left(\frac{\epsilon}{k} \right) C_{yz}^i \frac{\zeta Z'' \cos \theta}{2} - \left(\frac{\epsilon}{k} \right) C_{yT}^i \Omega \left(Z' + \frac{Z'''}{4} \right),$$

$$D_{yz} = -i [C_{yx}^e KU_{e0z} \sin \theta + C_{yz}^e (\Omega - KU_{e0x} \sin \theta)] \quad (\text{B.118})$$

$$- i C_{yx}^i \frac{\zeta Z'' \sin \theta \cos \theta}{2} - i C_{yz}^i \left(\zeta Z + \frac{\zeta Z'' \cos^2 \theta}{2} \right) - i C_{yT}^i \Omega \cos \theta \left(2Z' + \frac{Z'''}{4} \right),$$

$$D_{zx} = -K^2 \sin \theta \cos \theta - C_{zx}' (\Omega - KU_{e0z} \cos \theta) - C_{zz}' KU_{e0x} \cos \theta \quad (\text{B.119})$$

$$- C_{zx}^i \left(\zeta Z + \frac{\zeta Z'' \sin^2 \theta}{2} \right) - C_{zz}^i \frac{\zeta Z'' \cos \theta \sin \theta}{2} - C_{zT}^i \Omega \sin \theta \left(2Z' + \frac{Z'''}{4} \right),$$

$$D_{zy} = C_{zy}' \frac{\alpha^\times}{\omega_{ce} \tau_{ei}} \zeta Z + i C_{zy}' [\Omega - K(U_{e0x} \sin \theta + U_{e0z} \cos \theta)] \quad (\text{B.120})$$

$$+ i \left(\frac{\epsilon}{k} \right) C_{zx}^i \frac{\zeta Z'' \sin \theta}{2} + i \left(\frac{\epsilon}{k} \right) C_{zz}^i \frac{\zeta Z'' \cos \theta}{2} + i \left(\frac{\epsilon}{k} \right) C_{zT}^i \Omega \left(Z' + \frac{Z'''}{4} \right),$$

$$D_{zz} = K^2 \sin^2 \theta - C_{zx}' KU_{e0z} \sin \theta - C_{zz}' (\Omega - KU_{e0x} \sin \theta) \quad (\text{B.121})$$

$$- C_{zx}^i \frac{\zeta Z''}{2} \sin \theta \cos \theta - C_{zz}^i \left(\zeta Z + \frac{\zeta Z'' \cos^2 \theta}{2} \right) - C_{zT}^i \Omega \cos \theta \left(2Z' + \frac{Z'''}{4} \right),$$

Collisional effects on lower hybrid drift waves

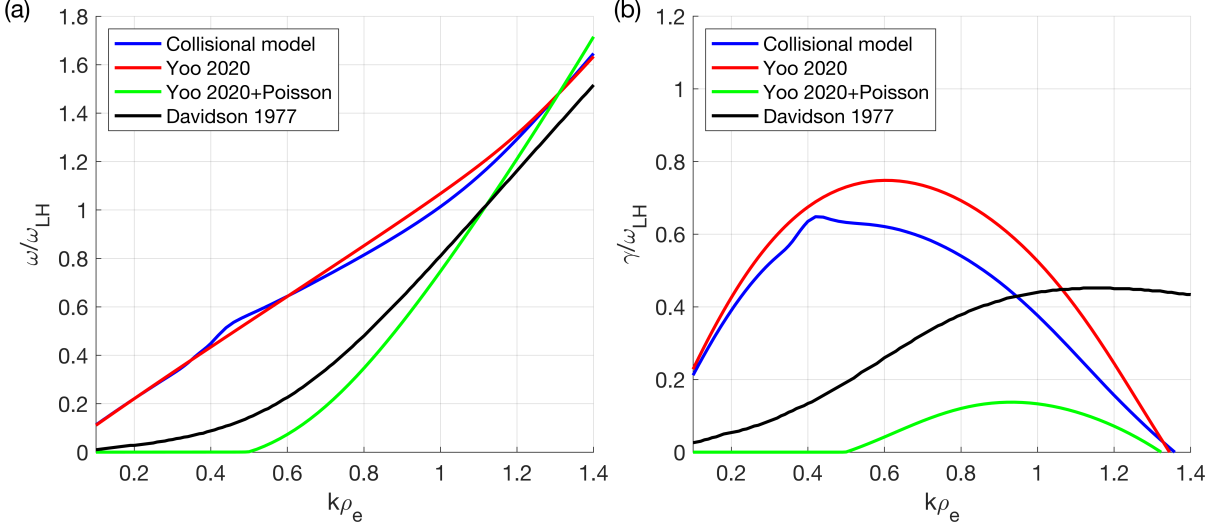


FIG. 8. Dispersion relation for the case of the ES-LHDW ($T_e = T_i = 10$ eV, $n_e = 2 \times 10^{13}$ cm $^{-3}$, $B_0 = 180$ Gauss, $u_{e0x} = 50$ km/s, singly-ionized helium). (a) Dispersion relation for four cases. The blue and red lines indicate results from collisional and collisionless models, respectively. The green line denotes the case derived here with Poisson's equation and perturbed quantities in the collisionless model. The black lines indicate results from the classical models¹⁷. (b) Growth rate of the ES-LHDW for all cases.

where

$$C_{xx}^i = 1 + C_{xx}^e \bar{c}_{ixx} + C_{xz}^e \bar{c}_{izx}, \quad (\text{B.122})$$

$$C_{xz}^i = C_{xx}^e \bar{c}_{ixz} + C_{xz}^e \bar{c}_{izz}, \quad (\text{B.123})$$

$$C_{xT}^i = C_{xx}^e \bar{c}_{ixT} + C_{xz}^e \bar{c}_{izT}, \quad (\text{B.124})$$

$$C_{yx}^i = C_{yx}^e \bar{c}_{ixx} + C_{yz}^e \bar{c}_{izx}, \quad (\text{B.125})$$

$$C_{yz}^i = C_{yx}^e \bar{c}_{ixz} + C_{yz}^e \bar{c}_{izz}, \quad (\text{B.126})$$

$$C_{yT}^i = C_{yx}^e \bar{c}_{ixT} + C_{yz}^e \bar{c}_{izT}, \quad (\text{B.127})$$

$$C_{zx}^i = C_{zx}^e \bar{c}_{ixx} + C_{zz}^e \bar{c}_{izx}, \quad (\text{B.128})$$

$$C_{zz}^i = 1 + C_{zx}^e \bar{c}_{ixz} + C_{zz}^e \bar{c}_{izz}, \quad (\text{B.129})$$

$$C_{zT}^i = C_{zx}^e \bar{c}_{ixT} + C_{zz}^e \bar{c}_{izT}. \quad (\text{B.130})$$

Appendix C: Comparison with Classical Model

Since the current model has been established independently, benchmarking with the classical model is desirable. Here, we used the well-known model by Davidson *et al.*¹⁷. For this benchmarking, we set both k_{\parallel} and u_{e0z} to be zero as in the classical model.

As shown in Fig. 8, results from both collisional (blue line) and collisionless (red line) models do not agree with results from the classical model (black line). In particular, our models expect an almost linear dispersion relation, but ω increases slowly for small $k\rho_e$ in the classical model. Another interesting difference is that the peak growth rate occurs around $k\rho_e \sim 0.6$ in our models, while it is around $k\rho_e \sim 1$ in the classical model. This discrepancy is not due to the choice of our heat flux closures; there is not much difference between our two models, which shows the insensitivity of the dispersion to p_{e1}^{\perp} . Moreover, the dispersion relation is independent of p_{e1}^{\parallel} when $k_{\parallel} = 0$. We also have confirmed that this discrepancy is not due to the inclusion of the perturbed ion current density, which is ignored in the classical model.

We note that the basic set of equations used in the classical model by Davidson *et al.*¹⁷ is different. The biggest difference is that Poisson's equation is used in the classical model, while we used Faraday's induction law. To understand the cause of this discrepancy, we have developed another model to calculate the dispersion relation. In this model, we follow basic equations of the classical model, while using our results for the perturbed density and current density.

In our geometry, the first order equations in Davidson *et al.*¹⁷ can be written as

$$E_{1y} - \frac{i\mu_0\omega}{k^2(1-\Delta^2)} J_{1y} = 0, \quad (\text{C.1})$$

$$E_{1x} + \frac{ie}{\epsilon_0 k} (n_{i1} - n_{e1}) = 0, \quad (\text{C.2})$$

where $\Delta = \omega/(ck)$, which is from the displacement current. This contribution is ignored, since the phase velocity of LHDWs is much smaller than the speed of light ($|\Delta^2| \ll 1$). We have confirmed that the dispersion relation is insensitive to the inclusion of Δ^2 .

For J_{1y} , n_{i1} , and n_{e1} , we use results from our models. The perturbed ion density is given by²⁴

$$n_{i1} = i \frac{n_0 e}{m_i k^2 v_{ti}^2} Z' (k E_{1x} - i \epsilon E_{1y}). \quad (\text{C.3})$$

For the perturbed electron density, we will use one from the collisionless model for simplicity, as there is not much difference between two models. We also assume that $T_{e0} = T_{i0}$. With $k_{\parallel} = 0$ and

Collisional effects on lower hybrid drift waves

$u_{e0z} = 0$, n_{e1} can be expressed as⁷

$$n_{e1} = \frac{kn_0}{(\omega - ku_{e0x})B_0} \left[iC_x^n E_{1x} + C_y^n \left(1 - \frac{ku_{e0x}}{\omega} \right) E_{1y} \right], \quad (\text{C.4})$$

where

$$C_x^n = \left(\alpha_e + \frac{\epsilon}{k} \right) \left[1 - \alpha_e^2 + \frac{1}{2\alpha_e} \left(\frac{\epsilon k v_{te}^2}{\omega_{ce}^2} + \frac{ku_{e0x}}{\omega_{ce}} \right) + \frac{1}{2} \left(\frac{k^2 v_{te}^2}{\omega_{ce}^2} + \frac{\epsilon u_{e0x}}{\omega_{ce}} \right) \right]^{-1}, \quad (\text{C.5})$$

$$C_y^n = \left(1 + \frac{\epsilon}{k} \alpha_e \right) \left[1 - \alpha_e^2 + \frac{1}{2\alpha_e} \left(\frac{\epsilon k v_{te}^2}{\omega_{ce}^2} + \frac{ku_{e0x}}{\omega_{ce}} \right) + \frac{1}{2} \left(\frac{k^2 v_{te}^2}{\omega_{ce}^2} + \frac{\epsilon u_{e0x}}{\omega_{ce}} \right) \right]^{-1}. \quad (\text{C.6})$$

The y component of the perturbed ion current is²⁴

$$J_{1y}^i = -\frac{ie^2 n_0}{m_i \omega} \zeta Z E_{1y}. \quad (\text{C.7})$$

The y component of the perturbed electron current is⁷

$$J_{1y}^e = -\frac{ien_0}{B_0} \left[iC_x^u E_{1x} + C_y^u \left(1 - \frac{ku_{e0x}}{\omega} \right) E_{1y} \right], \quad (\text{C.8})$$

where

$$C_x^u = \left(1 + \frac{ku_{e0x}}{2\alpha_e \omega_{ce}} \right) \left[1 - \alpha_e^2 + \frac{1}{2\alpha_e} \left(\frac{\epsilon k v_{te}^2}{\omega_{ce}^2} + \frac{ku_{e0x}}{\omega_{ce}} \right) + \frac{1}{2} \left(\frac{k^2 v_{te}^2}{\omega_{ce}^2} + \frac{\epsilon u_{e0x}}{\omega_{ce}} \right) \right]^{-1}, \quad (\text{C.9})$$

$$C_y^u = \left(\alpha_e - \frac{k^2 v_{te}^2}{2\alpha_e \omega_{ce}^2} \right) \left[1 - \alpha_e^2 + \frac{1}{2\alpha_e} \left(\frac{\epsilon k v_{te}^2}{\omega_{ce}^2} + \frac{ku_{e0x}}{\omega_{ce}} \right) + \frac{1}{2} \left(\frac{k^2 v_{te}^2}{\omega_{ce}^2} + \frac{\epsilon u_{e0x}}{\omega_{ce}} \right) \right]^{-1}. \quad (\text{C.10})$$

With Eqns. C.3, C.4, C.7, and C.8, Eqns. C.1 and C.2 can be written as

$$D_{yy} E_{1y} + D_{yx} E_{1x} = 0, \quad (\text{C.11})$$

$$D_{xy} E_{1y} + D_{xx} E_{1x} = 0, \quad (\text{C.12})$$

where

$$D_{yy} = 1 - \frac{\zeta Z}{K^2(1 - \Delta^2)} - \frac{\Omega - KU_{e0x}}{K^2(1 - \Delta^2)} C_y^u, \quad (\text{C.13})$$

$$D_{yx} = -\frac{i\Omega C_x^u}{K^2(1 - \Delta^2)}, \quad (\text{C.14})$$

$$D_{xy} = \frac{id_{\text{I}}^2}{2K^2 \lambda_{\text{Di}}^2} \left(\frac{\epsilon}{k} \right) Z' - \frac{i\omega_{\text{pi}}^2 C_y^n}{\omega_{\text{ci}}^2 \Omega}, \quad (\text{C.15})$$

$$D_{xx} = 1 - \frac{d_{\text{I}}^2}{2K^2 \lambda_{\text{Di}}^2} Z' + \frac{\omega_{\text{pi}}^2 C_x^n}{\omega_{\text{ci}}^2 (\Omega - KU_{e0x})}, \quad (\text{C.16})$$

where $\lambda_{\text{Di}} = \sqrt{\epsilon_0 T_{i0}/e^2 n_0}$ is the ion Debye Length. The dispersion relation can be obtained by setting $D_{xx}D_{yy} - D_{xy}D_{yx} = 0$.

The dispersion relation from this simplified model (green line) agrees with the classical model, as shown in Fig. 8 (a). This means that the discrepancy is due to the use of Poisson's equation, where the Faraday induction term is ignored. With the parameters for the ES-LHDW, β_e is about 0.25, which means that perturbed magnetic field due to the perturbed plasma current may not be negligible. This argument is supported by observations in laboratory and space^{7,10}, where magnetic field fluctuations exist when there are strong electric field fluctuations associated with ES-LHDW.

It is interesting to see that the growth rate from the simplified model is considerably lower than that from the classical model, as shown in Fig. 8 (b). This difference is likely related to the lack of a rigorous modeling of the heat flux in this simplified model. Although the magnitude is different, both models show that the peak growth rate is around $k\rho_e \sim 1$.

This comparison shows that the use of electron fluid equations are acceptable for dynamics of LHDWs. It should be also noted that only our models include full electromagnetic effects, since the induction term is included. These effects are important when β is not negligible.

ACKNOWLEDGMENTS

This work is supported by DOE Contract No. DE-AC0209CH11466, a NASA grant NNH20ZDA001N, NNSFC contract No. 11975163, the Priority Academic Program Development of Jiangsu Higher Education Institutions (PAPD), and a DOE grant DE-FG02-04ER54746. Digital data used are available in the DataSpace of Princeton University (<http://arks.princeton.edu/ark:/88435/dsp01x920g025r>).

DATA AVAILABILITY

The data that support the findings of this study are openly available in the DataSpace of Princeton University <http://arks.princeton.edu/ark:/88435/dsp01b2773z812>³⁸.

REFERENCES

¹S. D. Bale, F. S. Mozer, and T. Phan, “Observation of lower hybrid drift instability in the diffusion region at a reconnecting magnetopause,” *Geophys. Res. Lett.* **29**, 2180 (2002).

²C. Norgren, A. Vaivads, Y. V. Khotyaintsev, and M. André, “Lower hybrid drift waves: Space observations,” *Phys. Rev. Lett.* **109**, 055001 (2012).

³D. B. Graham, Y. V. Khotyaintsev, C. Norgren, A. Vaivads, M. André, S. Toledo-Redondo, P.-A. Lindqvist, G. T. Marklund, R. E. Ergun, W. R. Paterson, D. J. Gershman, B. L. Giles, C. J. Pollock, J. C. Dorelli, L. A. Avanov, B. Lavraud, Y. Saito, W. Magnes, C. T. Russell, R. J. Strangeway, R. B. Torbert, and J. L. Burch, “Lower hybrid waves in the ion diffusion and magnetospheric inflow regions,” *J. Geophys. Res.* **122**, 517–533 (2017), 2016JA023572.

⁴D. B. Graham, Y. V. Khotyaintsev, C. Norgren, A. Vaivads, M. André, J. F. Drake, J. Egedal, M. Zhou, O. Le Contel, J. M. Webster, B. Lavraud, I. Kacem, V. Génot, C. Jacquey, A. C. Rager, D. J. Gershman, J. L. Burch, and R. E. Ergun, “Universality of lower hybrid waves at earth’s magnetopause,” *Journal of Geophysical Research: Space Physics* **124**, 8727–8760 (2019), <https://agupubs.onlinelibrary.wiley.com/doi/pdf/10.1029/2019JA027155>.

⁵L.-J. Chen, S. Wang, M. Hesse, R. E. Ergun, T. Moore, B. Giles, N. Bessho, C. Russell, J. Burch, R. B. Torbert, K. J. Genestreti, W. Paterson, C. Pollock, B. Lavraud, O. Le Contel, R. Strangeway, Y. V. Khotyaintsev, and P.-A. Lindqvist, “Electron diffusion regions in magnetotail reconnection under varying guide fields,” *Geophysical Research Letters* **46**, 6230–6238 (2019), <https://agupubs.onlinelibrary.wiley.com/doi/pdf/10.1029/2019GL082393>.

⁶L.-J. Chen, S. Wang, O. Le Contel, A. Rager, M. Hesse, J. Drake, J. Dorelli, J. Ng, N. Bessho, D. Graham, L. B. Wilson, T. Moore, B. Giles, W. Paterson, B. Lavraud, K. Genestreti, R. Nakamura, Y. V. Khotyaintsev, R. E. Ergun, R. B. Torbert, J. Burch, C. Pollock, C. T. Russell, P.-A. Lindqvist, and L. Avanov, “Lower-hybrid drift waves driving electron nongyrotropic heating and vortical flows in a magnetic reconnection layer,” *Phys. Rev. Lett.* **125**, 025103 (2020).

⁷J. Yoo, J.-Y. Ji, M. V. Ambat, S. Wang, H. Ji, J. Lo, B. Li, Y. Ren, J. Jaramonte, L.-J. Chen, W. Fox, M. Yamada, A. Alt, and A. Goodman, “Lower hybrid drift waves during guide field reconnection,” *Geophysical Research Letters* **47**, e2020GL087192 (2020), [e2020GL087192](https://agupubs.onlinelibrary.wiley.com/doi/10.1029/2020GL087192) 10.1029/2020GL087192, <https://agupubs.onlinelibrary.wiley.com/doi/pdf/10.1029/2020GL087192>.

⁸T. A. Carter, H. Ji, F. Trintchouk, M. Yamada, and R. M. Kulsrud, “Measurement of lower-hybrid drift turbulence in a reconnecting current sheet,” *Phys. Rev. Lett.* **88**, 015001 (2001).

⁹H. Ji, S. Terry, M. Yamada, R. Kulsrud, A. Kuritsyn, and Y. Ren, “Electromagnetic fluctuations during fast reconnection in a laboratory plasma,” *Phys. Rev. Lett.* **92**, 115001 (2004).

¹⁰J. Yoo, M. Yamada, H. Ji, J. Jara-Almonte, C. E. Myers, and L.-J. Chen, “Laboratory study of magnetic reconnection with a density asymmetry across the current sheet,” *Phys. Rev. Lett.* **113**, 095002 (2014).

¹¹P. H. Yoon and A. T. Y. Lui, “Lower-hybrid-drift and modified-two-stream instabilities in current sheet equilibrium,” *J. Geophys. Res.* **109**, A02210 (2004), a02210.

¹²R. Kulsrud, *Plasma physics for astrophysics* (Princeton University Press, Princeton, 2005).

¹³I. Silin, J. Büchner, and A. Vaivads, “Anomalous resistivity due to nonlinear lower-hybrid drift waves,” *Physics of Plasmas* **12**, 062902 (2005), <https://doi.org/10.1063/1.1927096>.

¹⁴P. H. Yoon and A. T. Y. Lui, “Anomalous resistivity by fluctuation in the lower-hybrid frequency range,” *Journal of Geophysical Research: Space Physics* **112** (2007), 10.1029/2006JA012209, <https://agupubs.onlinelibrary.wiley.com/doi/pdf/10.1029/2006JA012209>.

¹⁵V. Roytershteyn, W. Daughton, H. Karimabadi, and F. S. Mozer, “Influence of the lower-hybrid drift instability on magnetic reconnection in asymmetric configurations,” *Phys. Rev. Lett.* **108**, 185001 (2012).

¹⁶V. Roytershteyn, S. Dorfman, W. Daughton, H. Ji, M. Yamada, and H. Karimabadi, “Electromagnetic instability of thin reconnection layers: Comparison of three-dimensional simulations with mrx observations,” *Phys. Plasmas* **20**, 061212 (2013).

¹⁷R. Davidson, N. Gladd, C. Wu, and J. Huba, “Effects of finite plasma beta on the lower-hybrid drift instability,” *Phys. Fluids* **20**, 301 (1977).

¹⁸L. Spitzer, *Physics of fully ionized gases*, 2nd ed. (Interscience Publishers, New York, USA, 1962).

¹⁹A. Kuritsyn, M. Yamada, S. Gerhardt, H. Ji, R. Kulsrud, and Y. Ren, “Measurements of the parallel and transverse spitzer resistivities during collisional magnetic reconnection,” *Phys. Plasmas* **13**, 055703 (2006).

²⁰J. Yoo, M. Yamada, H. Ji, J. Jara-Almonte, and C. E. Myers, “Bulk ion acceleration and particle heating during magnetic reconnection in a laboratory plasma,” *Phys. Plasmas* **21**, 055706 (2014).

²¹W. Daughton, “Electromagnetic properties of the lower-hybrid drift instability in a thin current sheet,” *Phys. Plasmas* **10**, 3103–3119 (2003).

²²W. Daughton, G. Lapenta, and P. Ricci, “Nonlinear Evolution of the Lower-Hybrid Drift Instability in a Current Sheet,” *Phys. Rev. Lett.* **93**, 105004 (2004).

²³X. Y. Wang, Y. Lin, L. Chen, and Z. Lin, “A particle simulation of current sheet instabilities under finite guide field,” *Physics of Plasmas* **15**, 072103 (2008), <https://doi.org/10.1063/1.2938732>.

²⁴H. Ji, R. Kulsrud, W. Fox, and M. Yamada, “An obliquely propagating electromagnetic drift instability in the lower hybrid frequency range,” *J. Geophys. Res.* **110**, A08212 (2005).

²⁵J.-Y. Ji and I. Joseph, “Electron parallel closures for the 3 + 1 fluid model,” *Phys. Plasmas* **25**, 032117 (2018), <https://doi.org/10.1063/1.5014996>.

²⁶J.-Y. Ji and E. D. Held, “Closure and transport theory for high-collisionality electron-ion plasmas,” *Physics of Plasmas* **20**, 042114 (2013), <https://doi.org/10.1063/1.4801022>.

²⁷N. Krall and P. Liewer, “Low-frequency instabilities in magnetic pulses,” *Phys. Rev. A* **4**, 2094 (1971).

²⁸N. Gladd, “The Lower Hybrid Drift Instability and the Modified Two Stream Instability in High Density Theta Pinch Environments,” *Plasma Physics* **18**, 27 (1976).

²⁹G. W. Hammett and F. W. Perkins, “Fluid moment models for Landau damping with application to the ion-temperature-gradient instability,” *Phys. Rev. Lett.* **64**, 3019–3022 (1990).

³⁰S. I. Braginskii, “Transport processes in a plasma,” in *Reviews of Plasma Physics*, Vol. 1, edited by M. A. Leontovich (Consultants Bureau, New York, USA, 1965) pp. 205–311.

³¹F. Trintchouk, M. Yamada, H. Ji, R. M. Kulsrud, and T. A. Carter, “Measurement of the transverse spitzer resistivity during collisional magnetic reconnection,” *Phys. Plasmas* **10**, 319–322 (2003).

³²W. Fox, F. Sciortino, A. v. Stechow, J. Jara-Almonte, J. Yoo, H. Ji, and M. Yamada, “Experimental verification of the role of electron pressure in fast magnetic reconnection with a guide field,” *Phys. Rev. Lett.* **118**, 125002 (2017).

³³K. Tummel, L. Chen, Z. Wang, X. Y. Wang, and Y. Lin, “Gyrokinetic theory of electrostatic lower-hybrid drift instabilities in a current sheet with guide field,” *Physics of Plasmas* **21**, 052104 (2014), <https://doi.org/10.1063/1.4875720>.

³⁴J. Yoo, B. Na, J. Jara-Almonte, M. Yamada, H. Ji, V. Roytershteyn, M. R. Argall, W. Fox, and L.-J. Chen, “Electron heating and energy inventory during asymmetric reconnection in a laboratory plasma,” *J. Geophys. Res.* **122**, 9264–9281 (2017), 2017JA024152.

³⁵Y. Hu, J. Yoo, H. Ji, A. Goodman, and X. Wu, “Probe measurements of electric field and electron density fluctuations at megahertz frequencies using in-shaft miniature circuits,” *Review of Scientific Instruments* **92**, 033534 (2021), <https://doi.org/10.1063/5.0035135>.

³⁶F. S. Mozer, M. Wilber, and J. F. Drake, “Wave associated anomalous drag during magnetic field reconnection,” *Phys. Plasmas* **18**, 102902 (2011).

Collisional effects on lower hybrid drift waves

³⁷J.-Y. Ji and E. D. Held, “Landau collision operators and general moment equations for an electron-ion plasma,” Physics of Plasmas **15**, 102101 (2008), <https://doi.org/10.1063/1.2977983>.

³⁸Dataset: J. Yoo, “Effects of coulomb collisions on lower hybrid drift waves inside a laboratory reconnection current sheet,” DataSpace of Princeton University (2021), <https://dataspace.princeton.edu/handle/88435/dsp01x920g025r>.